UHASSELT
KNOWLEDGE IN ACTION

Maastricht University

Faculty of Medicine and Life Sciences
School for Life Sciences
Master of Biomedical Sciences

Masterthesis

Microdomain-specific beta-adrenergic regulation of calcium signaling in tachycardia-induced atrial fibrillation

Anne Cuypers

Thesis presented in fulfillment of the requirements for the degree of Master of Biomedical Sciences, specialization Clinical Molecular Sciences

SUPERVISOR :
Prof. Dr. Gudrun ANTOONS

MENTOR :
drs. Patrick SCHÖNLEITNER

2017
2018

Transnational University Limburg is a unique collaboration of two universities in two countries: the University of Hasselt and Maastricht University.

UHASSELT
KNOWLEDGE IN ACTION

www.uhasselt.be
Universiteit Hasselt
Campus Hasselt:
Martelarenlaan 42 | 3500 Hasselt
Campus Diepenbeek:
Agoralaan Gebouw D | 3590 Diepenbeek

UHASSELT
KNOWLEDGE IN ACTION

Maastricht University

Faculty of Medicine and Life Sciences
School for Life Sciences
Master of Biomedical Sciences

Masterthesis

Microdomain-specific beta-adrenergic regulation of calcium signaling in tachycardia-induced atrial fibrillation

Anne Cuypers

Thesis presented in fulfillment of the requirements for the degree of Master of Biomedical Sciences, specialization Clinical Molecular Sciences

SUPERVISOR :
Prof. Dr. Gudrun ANTOONS

MENTOR :
drs. Patrick SCHÖNLEITNER

Table of contents

Acknowledgements

As a biomedical researcher, I learned a lot, both practical skills and theoretical knowledge. Besides, I got to know many new people who became good friends. During the last eight months, I conducted my senior internship at the Physiology department at Maastricht University. The time that I spent here in Maastricht can be summarized as wonderful, instructive and inspiring to me. Without the help of several people, this thesis could not have succeeded. Therefore, I would like to express my gratitude.

First and foremost, I would like to express my sincere gratitude to my promotor, Prof. Dr. Gudrun Antoons for realizing this project, for reviewing my report, as well as for the continuous support, enthusiasm, and motivation she gave me. Her passion, knowledge, and criticism inspired me to further explore scientific research. I would also like to thank you for all the opportunities that you gave me during this internship. I simply could not wish for a better promotor!

I would like to offer my special thanks to my daily supervisor Patrick Schönleitner, to guide me during the experimental work. Thank you for giving me the responsibility to plan my own experiments and to work independently in the lab. I really enjoyed our scientific and less scientific conversations. You were always ready to answer my questions, to give me advice, and to support me with good coffee. I wish you the best with the rest of your career!

Next, I would like to pay tribute to Giulia Gatta and Vladimir Sobota, who have supported me with their friendship and their sense of humor. Thank you for the countless memorable moments!

A word of appreciation goes to all the members of the Physiology group for creating a pleasant working atmosphere and for helping me in any way possible. I wish to acknowledge the help provided by Marion Kuiper for the pacemaker lead implantations. Also, many thanks to Helma Kuijpers and Kevin Knoops for the help with the confocal microscope.

Furthermore, advices, coffee breaks, and lunches shared with colleagues and fellow students have also been a great help to succeed this internship and to make thesis writing a pleasure.

Finally, I would like to thank my parents, my boyfriend, my family, and my friends for the continuous support during my education and for giving me the opportunity to pursue my dreams!

List of abbreviations

AC	adenylyl cyclase
AF	atrial fibrillation
AM	atrial myocytes
AP	action potential
AT	axial tubules
Ca^{2+}	calcium
CaMKII	Ca^{2+}/calmodulin-dependent protein kinase II
cAMP	cyclic adenosine monophosphate
CaT	calcium transient
CICR	calcium-induced calcium release
DAD	delayed afterdepolarizations
EAD	early afterdepolarizations
EC	excitation-contraction
Epac	exchange protein directly activated by cAMP
HF	heart failure
ICaL	L-type Ca^{2+} current
INa^{+}	sodium current
ISO	Isoproterenol
LTCC	L-type Ca^{2+} channels
NCX	Na/Ca^{2+} exchanger
NOS1	nitric oxide synthase 1
PBS	phosphate buffered saline
PLB	phospholamban
PFA	paraformaldehyde
PKA	protein kinase A
RAP	rapid atrial pacing
ROI	region of interest
RyR	ryanodine receptors
SERCA	sarco/endoplasmic reticulum Ca^{2+}-ATPase
SR	sarcoplasmic reticulum
SS	subsarcolemmal
TAT	transverse-axial tubules
TT	transverse tubules
TTP	time to peak
UC	uncoupled
WGA	wheat germ agglutinin

Abstract

Introduction: Atrial fibrillation (AF) is the most common cardiac arrhythmia and is associated with increasing morbidity and mortality. B-adrenergic stimulation increases AF susceptibility. In atrial myocytes (AM), abnormalities in Ca^{2+} release from the sarcoplasmic reticulum are related to dysregulation of ryanodine receptors (RyR) contributing to contractile dysfunction and arrhythmia generation. Subcellularly, RyR-mediated Ca^{2+} release is heterogeneous with sites of slow release (uncoupled RyR) and fast release (RyR near axial membranes and sarcolemma), suggesting microdomain-specific-phosphorylation of RyR. To our knowledge, no studies have been performed to investigate microdomain-specific protein kinase A (PKA)-dependent-phosphorylation of dysregulated RyR during β-adrenergic modulation in AF.

Materials & methods: AM from sham-operated- (SHAM) and rapid atrial paced (RAP; 5 days at 10 Hz) rabbits were stimulated under baseline (Normal Tyrode) or after β-adrenergic stimulation (Isoproterenol, 300 nM). Ca^{2+} transients were measured confocally in fluo-4 acetoxymethyl ester loaded cells during field stimulation (1 Hz, 37 °C). PKA-dependent RyR phosphorylation was analyzed by immunostaining and assigned to the nearest membrane. Confocal images were analyzed using Fiji (ImageJ). Statistical significance ($p<0.05$) was evaluated with Student's t-test, Mann-Whitney U test, or ANOVA.

Results: In atrial RAP cells, the amplitude of baseline Ca^{2+} transients was significantly reduced, but normalized after β-adrenergic stimulation. Similarly, global RyR phosphorylation was reduced in RAP cells but showed a greater relative increase after β-adrenergic stimulation. Subcellularly, baseline RyR phosphorylation in SHAM cells was relatively higher at axial tubules (AT) and subsarcolemmal; β-adrenergic stimulation shifted the frequency distributions to the right; this shift was most pronounced for RyR phosphorylation at the uncoupled. In RAP cells at microdomain level, β-adrenergic rescue of RyR phosphorylation involved equal recruitment of RyR at uncoupled, subsarcolemmal and AT regions.

Discussion & conclusion: In AM, the level of PKA-dependent RyR phosphorylation depends on the subcellular location. Atrial remodeling due to rapid pacing causes RyR hypophosphorylation that can be reversed by β-adrenergic stimulation. This mechanism could, at least partly, contribute to the β-adrenergic rescue of Ca^{2+} transients in AF improving contractility, but could adversely increase the likelihood of arrhythmias.

Samenvatting

Inleiding: Atriale fibrillatie (AF) is de meest voorkomende hartritmestoornis en gaat gepaard met een toenemende morbiditeit en mortaliteit. B-adrenerge stimulatie verhoogt de vatbaarheid voor AF. In atriale myocyten (AM) zijn afwijkingen in Ca^{2+}-afgifte in het sarcoplasmatisch reticulum gerelateerd aan een ontregeling van de ryanodine-receptoren (RyR). Dit draagt bij tot contractiele dysfunctie en tot het genereren van hartritmestoornissen. Subcellulair is RyR-gemedieerde Ca^{2+}-afgifte heterogeen met plaatsen van langzame afgifte (ongekoppelde RyR) en snelle afgifte (RyR nabij axiale membranen en sarcolemma), wat wijst op microdomein-specifieke fosforylatie van RyR. Voor zover ons bekend is, zijn er nog geen studies uitgevoerd om microdomein-specifieke proteine kinase A (PKA)-afhankelijke fosforylatie van ontregelde RyR tijdens β-adrenerge modulatie in AF te onderzoeken.

Materialen & methoden: AM uit sham-geopereerde (SHAM) en uit snel atriaal-gepacete (RAP; 5 dagen op 10 Hz) konijnen werden gestimuleerd onder baseline (Normale Tyrode) of na β-adrenerge stimulatie (Isoproterenol, 300 nM). Ca^{2+}-transiënten werden confocaal gemeten in met fluo-4 acetoxymethyl ester geladen cellen tijdens veldstimulatie (1 Hz, 37 °C). PKA-afhankelijke RyR fosforylatie werd geanalyseerd door middel van immunokleuring en werd toegewezen aan het dichtstbijzijnde membraan. Confocale beelden werden geanalyseerd met behulp van Fiji (ImageJ). Statistische significantie ($p < 0,05$) werd geëvalueerd met Student's t-test, Mann-Whitney U-test of ANOVA.

Resultaten: In atriale RAP-cellen was de amplitude van de baseline Ca^{2+}-transiënten significant verminderd, maar werd genormaliseerd na β-adrenerge stimulatie. Op dezelfde manier was de globale RyR fosforylatie verminderd in RAP-cellen, maar vertoonde een grotere relatieve toename na β-adrenerge stimulatie. Subcellulair was de baseline RyR fosforylatie in SHAM-cellen relatief hoger bij axiale tubules (AT) en subsarcolemma; β-adrenerge stimulatie verschoof de frequentie distributie op naar rechts; de shift was het meest uitgesproken voor RyR fosforylatie bij ongekoppelde regio's. In RAP cellen op microdomein niveau omvatte de β-adrenerge redding van RyR fosforylatie gelijke rekrutering van RyR bij ongekoppelde, subsarcolemmale en AT-regio's.

Discussie en conclusie: In AM hangt het niveau van PKA-afhankelijke RyR fosforylatie af van de subcellulaire locatie. Atriale remodelering door snelle pacing veroorzaakt RyR hypofosforylatie die kan worden omgekeerd door β-adrenerge stimulatie. Dit mechanisme zou enerzijds kunnen bijdragen aan de β-adrenerge redding van Ca^{2+}-transiënten in AF om de contractiliteit te verbeteren, maar zou anderzijds de waarschijnlijkheid op aritmieën kunnen vergroten.

1 Introduction

1.1 Atrial fibrillation

Atrial fibrillation (AF) is the most common cardiac arrhythmia increasing in prevalence with age (1-3). AF can be defined as a supraventricular tachyarrhythmia with resultant atrial mechanical dysfunction (1, 4, 5). AF is associated with increased morbidity and mortality that is predominantly mediated by ischemic stroke, myocardial infarction and the progression of heart failure (HF) (4, 6). The pathophysiology of AF consists of three main stages: initiation, maintenance, and progression of the arrhythmia. Clinical episodes of AF can be classified into paroxysmal, persistent and chronic. In paroxysmal AF, the arrhythmia lasts for <7 days and is spontaneously converted into normal sinus rhythm. In persistent AF (≥7 days), the arrhythmia continues and requires an intervention (i.e. electrical or pharmacological) to restore sinus rhythm. When the arrhythmia is long-lasting (>1 year) and cannot be converted into regular sinus rhythm, the episode is classified as permanent or chronic (4, 6). The mechanisms causing AF are highly complex and depend on the stage of AF. AF itself promotes AF by inducing electrical, ionic and structural remodeling of the atria (7, 8). In addition, risk factors (i.e. age or gene mutations) and co-morbidities (i.e. HF or hypertension) play a role in the predisposition to AF through disease-specific remodeling resulting in arrhythmogenic substrates (5, 9). Modulating factors such as adrenergic stimulation are critical for inducing AF episodes, presumably through dysregulation of calcium (Ca^{2+}) handling (3, 10). Compelling evidence suggests a role for dysregulated Ca^{2+} in AF triggering mechanisms and substrate remodeling (4). Despite the clinical importance of AF (11), subcellular details of Ca^{2+} signaling, more specifically the effects of β-adrenergic stimulation on microdomain-specific Ca^{2+}release, are not completely understood.

1.2 Calcium signaling

1.2.1 General scheme of excitation-contraction coupling in cardiac myocytes

The heart is a muscle that contracts and pumps blood (12). It consists of specialized muscle cells called cardiac myocytes. The contraction of these cells is initiated by electrical impulses, known as action potentials. During each heartbeat, an action potential (AP) is initiated in the atria through activation of voltage-dependent cardiac Na^+ channels, producing a depolarizing current (INa^+) (4). The initiated AP triggers a transient increase in intracellular Ca^{2+}, the Ca^{2+} transient. The Ca^{2+} rise results from a small Ca^{2+} influx via L-type Ca^{2+} channels (LTCC), inducing a much larger amount of Ca^{2+} release from the sarcoplasmic reticulum (SR) through activation of ryanodine receptors (RyR), a process referred to as Ca^{2+}-induced Ca^{2+} release (CICR) (13). The close proximity of RyR near LTCC in invaginating transverse tubules (T-tubules; TT) is critical for efficient CICR. Subsequently, the cytosolic Ca^{2+} binds to the myofilaments causing contraction. When relaxation occurs, Ca^{2+} is mainly taken up again into the SR by a sarcoplasmic Ca^{2+}-ATPase (SERCA), and partly removed from the cytosol via the Na/Ca^{2+} exchanger (NCX). For proper cardiac function, well-coordinated Ca^{2+} release during excitation-contraction (EC) coupling is essential. The Ca^{2+} fluxes underlying EC coupling are illustrated in Figure 1A (13).

1.2.2 Effect of β-adrenergic stimulation on calcium signaling

B-adrenergic stimulation of protein kinase A (PKA) is known to enhance Ca^{2+} release (14, 15). A β-adrenergic agonist (e.g. Isoproterenol; ISO) binds to Gs protein-coupled adrenergic receptors (Figure 1B). This, in turn, will stimulate adenylyl cyclase (AC) and thereby increase cytosolic cyclic adenosine monophosphate (cAMP) levels. cAMP will activate PKA which is a common downstream effector of β-adrenergic signaling (14, 16, 17). PKA is responsible for the phosphorylation of LTCC and RyR, increasing Ca^{2+} current and sensitizing RyR, respectively (Figure 1B) (10, 13, 18, 19). SERCA activity is regulated by its inhibitor phospholamban (PLB). Phosphorylation of PLB by PKA during β-adrenergic stimulation relieves SERCA from PLB inhibition and increases SR Ca^{2+} re-uptake (Figure 1B) (13). Independent of PKA signaling, β-adrenergic stimulation activates Ca^{2+}/calmodulin-dependent protein kinase II (CaMKII) via Epac (exchange protein directly activated by cAMP) and/or nitric oxide synthase 1 (NOS1) activation (Supplemental figure 1) (19-21). CaMKII phosphorylates LTCC, RyR, and PLB at phosphorylation sites other than PKA (18, 22, 23) and further contributes to the inotropic and lusitropic effects of β-adrenergic stimulation on the Ca^{2+} transient.

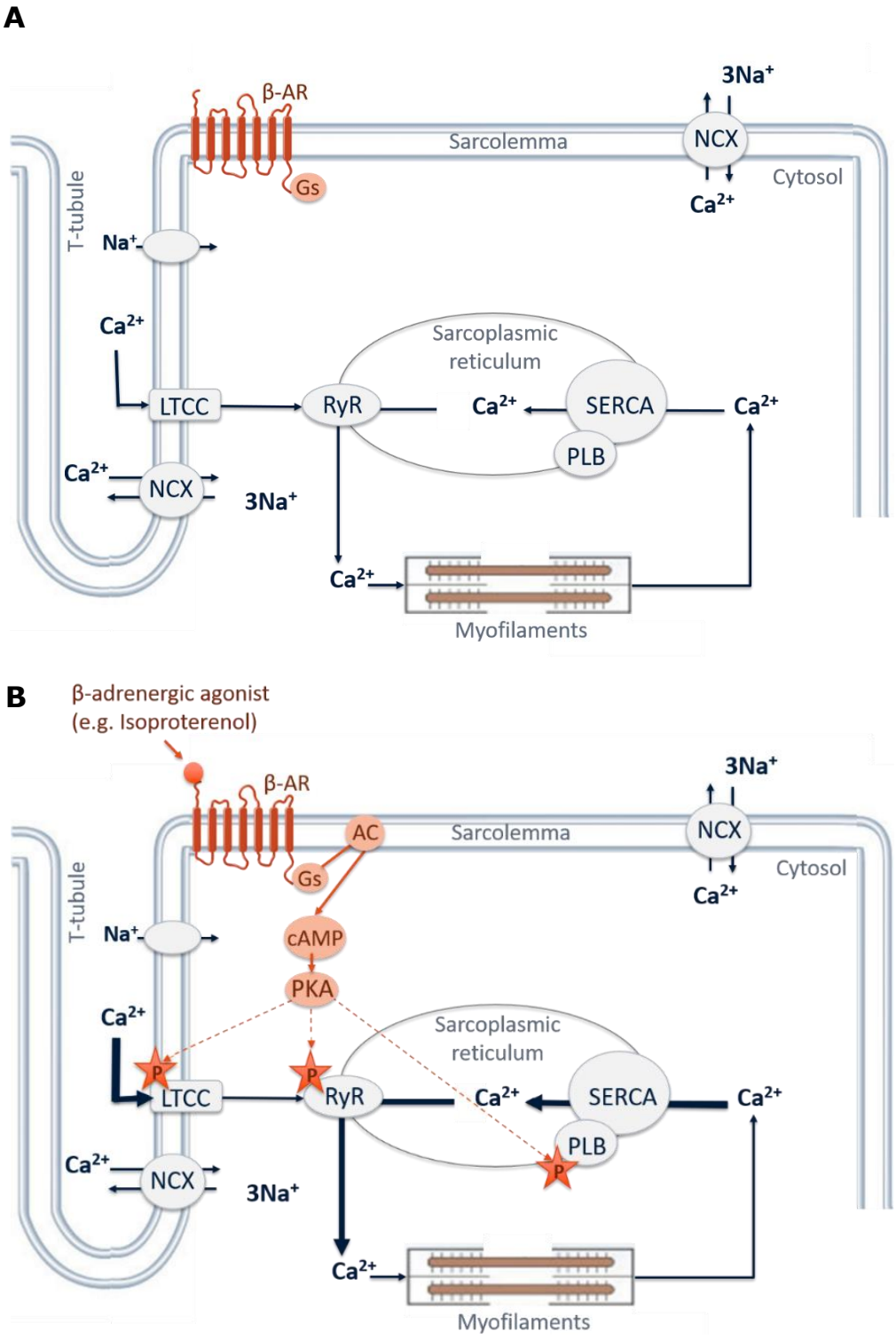

Figure 1 Subcellular structures involved in facilitating excitation-contraction coupling. *Calcium signaling* ***A,*** *at baseline and* ***B,*** *after PKA-dependent β-adrenergic stimulation. Asterisks with P indicate PKA-dependent phosphorylation. LTCC = L-type Ca^{2+}channel, NCX = Na/Ca^{2+} exchanger, β-AR = β-adrenergic receptor, AC = adenylyl cyclase, cAMP = cyclic adenosine monophosphate, PKA = protein kinase A, RyR = ryanodine receptor, SERCA = sarcoplasmic Ca^{2+}-ATPase, PLB = phospholamban.*

1.2.3 Ryanodine receptors

RyR are organized in clusters and located in the SR membrane. Activation of a RyR cluster produces a Ca^{2+} spark (24). RyR are activated by a rise in cytosolic Ca^{2+}, through Ca^{2+} influx via LTCC during CICR, or via propagating Ca^{2+} release from neighboring RyR. The latter occurs during spontaneous Ca^{2+} release during diastole (see paragraph 1.3), or when RyR are not coupled to LTCC (see paragraph 1.5). To ensure tight control of CICR, RyR Ca^{2+} sensitivity is highly regulated by phosphorylation. Biochemical data showed that the RyR channel consists of three major phosphorylation sites namely serine 2808, serine 2814, and serine 2030 (14). Serine 2808 is reported to be the key site on RyR for phosphorylation by PKA (25). PKA phosphorylation of RyR causes dissociation of calstabin2 (FKBP12.6) from the channel complex, thereby increasing open probability of the RyR channel (17). In response to β-adrenergic stimulation, activation of CaMKII by Epac, lead to phosphorylation of RyR at serine 2814, which is reported as the main phosphorylation site of CaMKII (16, 18, 22, 26, 27).

1.3 Mechanisms of AF

Ectopic triggered activity and re-entry are the two main mechanisms by which AF develops. Ectopic triggered activity is caused by early afterdepolarizations (EAD) and delayed afterdepolarizations (DAD). Re-entry can be defined as a continuous repetitive propagation of an excitatory wave (4). Functional (i.e. ion current) and structural (i.e. fibrosis) changes due to remodeling of the atria make patients susceptible to relapses by facilitating triggered activity in a vulnerable substrate. Furthermore, patients are prone to developing a permanent state of AF, in which re-entry is thought to play a role (4). For this project, the focus will be on the initiation/triggers of AF, i.e. EAD and/or DAD (Figure 2). EAD and DAD are both oscillations of the myocyte membrane potential which can cause abnormal spontaneous discharges generating focal ectopic triggered activity. EAD typically develop with prolonged repolarization and are caused by reactivation of LTCC (28) or late INa^+ (4, 28, 29), while DAD occur during diastole and are caused by abnormal SR Ca^{2+}release, either due to RyR dysfunction or by an excessive increase in SR Ca^{2+} load (11, 30). Spontaneous diastolic SR Ca^{2+}- release can activate NCX, resulting in a transient-inward current of three Na^+ ions while Ca^{2+} is extruded from the atrial cardiac myocyte. This inward current depolarizes the membrane potential and when reaching the threshold for excitation, an ectopic impulse will be generated (4). In conditions of AP shortening, as in AF, a large Ca^{2+}- release may cause DAD during late repolarization (4). In this particular case, the DAD are referred to as phase-3 EAD (4). B-adrenergic stimulation promotes both EAD and DAD, which is consequently to increased LTCC, SR Ca^{2+} gain, and RyR activity (Figure 2) (11, 31).

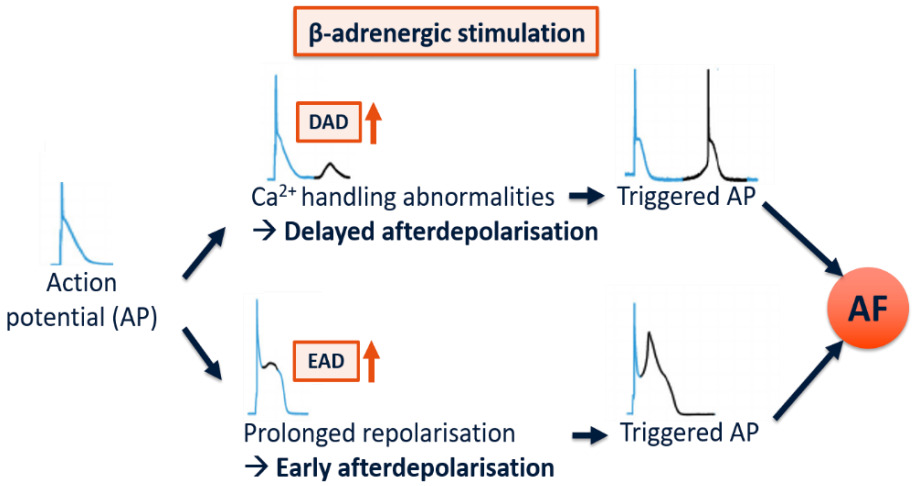

Figure 2 Triggers of ectopic activity. *Oscillations of the myocyte membrane potential (i.e. DAD and EAD) contribute to abnormal spontaneous discharges (triggered AP) which can initiate AF. B-adrenergic stimulation exerts promoting effects on DAD and EAD, contributing to AF. DAD = delayed afterdepolarizations, EAD = early afterdepolarizations, AP = action potential, AF = atrial fibrillation.*

1.4 Altered calcium signaling in AF

1.4.1 Baseline calcium signaling in AF

Atria that are rapidly paced, as in AF, are subjected to atrial electrical remodeling (32). There is considerable evidence that dysregulated Ca^{2+} homeostasis as a result of atrial remodeling plays a role in the pathogenesis of AF (32-35). Reduction of L-type Ca^{2+} current (ICaL), NCX upregulation, reduced Ca^{2+} transients, increased Ca^{2+} leak and altered SR function have all been reported and can contribute to the development of DAD (32, 34). Molecular mechanisms underlying afterdepolarizations depend on the model (i.e. how AF has been induced experimentally) and on the stage of AF. In humans with chronic AF, the high DAD incidence despite normal SR Ca^{2+} load has been explained by hyperactive RyR due to increased CaMKII phosphorylation in combination with increased NCX current destabilizing the membrane potential (35). At paroxysmal stages of human AF, NCX function is normal and DAD occurrence has been associated with an excessive increase in SR Ca^{2+} load related to PLB phosphorylation. RyR activity was also increased by an unknown mechanism but unrelated to CaMKII (36). As mentioned before, these mechanisms generate Ca^{2+} sparks that can contribute to the development of ectopic triggered activity.

1.4.2 Calcium signaling in AF during β-adrenergic stimulation

Modulation of Ca^{2+} signaling by β-adrenergic stimulation is known to be an important factor of AF initiation, but this factor is yet poorly understood (3, 4, 10). B-adrenergic stimulation induces arrhythmogenic activity in AF patients (37) and afterdepolarizations in atrial myocytes (AM) (38). As previously mentioned, β-adrenergic stimulation enhances Ca^{2+} release; SR Ca^{2+} loading via increased Ca^{2+} influx (PKA-dependent phosphorylation of LTCC) and SR Ca^{2+} uptake (PKA-dependent phosphorylation of PLB), and possibly RyR hyperphosphorylation (10, 14), are PKA-dependent mechanisms that would promote afterdepolarizations. In experimental and human AF, ICaL is mostly reduced. Interestingly, there are some data on the rescue of the ICaL and Ca^{2+} transient after β-adrenergic stimulation. Wagoner *et al.* (39) demonstrated that ICaL was lower in myocytes from chronic AF patients. Furthermore, they showed that this lowered ICaL was rescued in response to maximal β-adrenergic stimulation (Supplemental figure 2) (39). A study by Voigt *et al.* (35) observed 50% and 48% lower amplitudes of ICaL and AP-triggered Ca^{2+} transient, respectively, in chronic AF patients when compared to controls. However, the tendency of diastolic $[Ca^{2+}]i$ appeared to be higher in chronic AF patients than in controls. The higher diastolic $[Ca^{2+}]i$ was due to an enhanced SR Ca^{2+} leak through CaMKII-hyperphosphorylated RyR together with larger I_{NCX}, causing triggered activity in chronic AF patients (35).

1.5 Calcium Microdomains

In cardiac myocytes, a Ca^{2+} microdomain refers to a restricted space in which the generation and diffusion of Ca^{2+} signals are limited in time and space. (40). Ca^{2+} microdomains exist between junctional SR and invaginating tubular membrane structures and are referred to as dyads. In the dyad, LTCC are juxtaposed to clusters of RyR (specified as coupled RyR) and control their direct activation during CICR. Not all RyR are localized at dyads; uncoupled RyR are activated through propagated Ca^{2+} release with a delay. Recent evidence suggests that regulation of RyR release sites by kinases (CaMKII, PKA) is selective for coupled and uncoupled RyR (19, 41, 42). In myocytes, four different microdomains have been characterized: subsarcolemmal (SS), TT, axial tubules (AT) and uncoupled (UC) release sites (19, 42). Ventricular cardiac myocytes have a dense and regular network of TT. Loss of TT, as in HF, causes less efficient SR Ca^{2+} release (42). In the atria, the structural arrangement of the tubule network is remarkably different from the ventricle. Whilst TT are sparse, atrial cells have a large population of AT (42). A recent study by Brandenburg *et al.* (42) in healthy mice reported that AT form a distinct population of functional microdomains releasing Ca^{2+} faster due to AT-specific hyperphosphorylation of RyR. They also found that AT are subjected to remodeling in a mice model of HF-induced atrial remodeling. In line with these findings, our previous research in a rabbit model of tachypaced-induced atrial remodeling (rapid atrial pacing; RAP) showed that the fraction of AT was increased in relation to TT although the transverse-axial tubules (TAT) network density was lower in our RAP model compared to the SHAM group (Figure 3). The overall loss of TAT (Figure 3) also suggests a larger fraction of uncoupled RyR release sites in RAP (41).

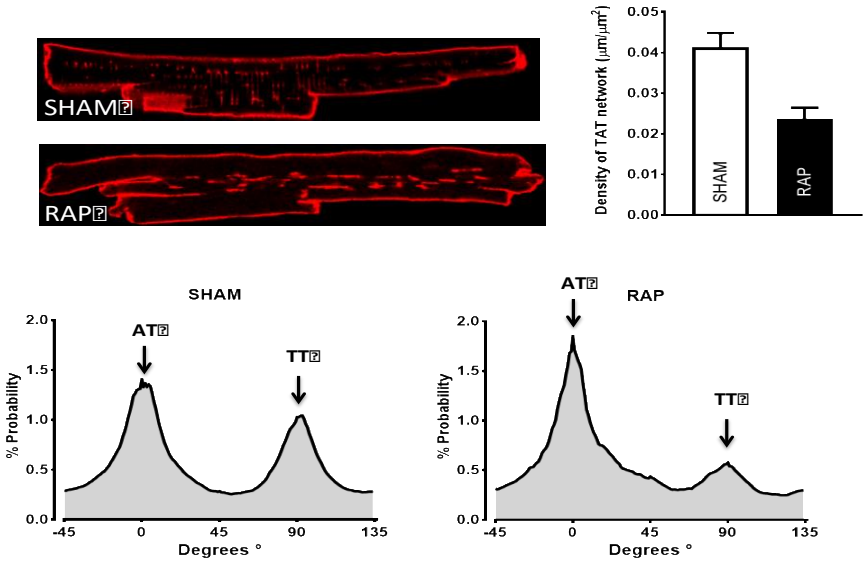

Figure 3 Remodeling of tubular membrane system in atrial fibrillation showing preferential loss of transverse tubules (TT) in RAP myocytes. *Membranes were stained with wheat germ agglutinin (WGA) (Schönleitner et al., unpublished). AT = axial tubules.*

1.6 Research aim

In AM, abnormalities in Ca^{2+} release from the SR are related to dysregulation of RyR contributing to contractile dysfunction and arrhythmia generation. Subcellularly, RyR-mediated Ca^{2+} release is heterogeneous with sites of slow release (uncoupled RyR) and fast release (RyR near axial membranes (TAT) and SS) (42, 43), suggesting microdomain-specific-phosphorylation of RyR. To our knowledge, no studies have been performed to explore microdomain-specific β-adrenergic PKA-dependent regulation of Ca^{2+} release in AF. The overall aim is to understand microdomain-specificity of β-adrenergic PKA-dependent modulation of Ca^{2+} release in a rabbit model of tachypaced-induced atrial remodeling (RAP). For this project, we made use of rabbits, as it is known that rabbit hearts are more similar to human in terms of Ca^{2+} handling than small rodents (13, 44). At the structural level, we investigated PKA-dependent RyR phosphorylation at AT, UC and SS sites. At the functional level, microdomain-specific Ca^{2+} transients were analyzed. We hypothesized that there are more phosphorylated RyR near AT and SS at baseline in SHAM-operated rabbits. Because there are relatively more uncoupled and axial release sites in RAP-rabbits due to remodeling, we further hypothesized that β-adrenergic modulation of Ca^{2+} release involves the recruitment of uncoupled and axial release sites. In view of our hypothesis, we formed three objectives. Our first objective was to investigate the global effect of β-adrenergic stimulation at the functional as well as at the structural level in RAP. Secondly, we investigated at baseline and after β-adrenergic stimulation whether microdomain-specific RyR phosphorylation was altered in RAP. The third objective was to correlate structural data of microdomain-specific in situ phosphorylation (i.e. triple immunostainings) with functional data (i.e. measurements of Ca^{2+} transients). With these three objectives, we aim to clarify microdomain-specificity of β-adrenergic stimulation on Ca^{2+} release in a RAP rabbit model.

2 Materials and methods

2.1 Animal model

New Zealand White rabbits (2.5-3.0 kg) were randomly allocated to a SHAM (n=9) or a RAP (n=10) group. All rabbits were anesthetized with ketamine (50 mg/kg) / xylazine (5 mg/kg) via intramuscular injection. After endotracheal intubation, anesthesia was maintained via inhalation of 0.5% isoflurane controlled by mechanical ventilation (rate of ~30/minute). A pacemaker lead was implanted via the left internal jugular vein into the right atrium (32). After a one week recovery period, the right atrium of the RAP group was rapidly paced (at 10 Hz) for 5 days (short-term) using an external pacemaker (Itrel Medtronic, 4x threshold). Anesthetized (ketamine (50 mg/kg) / xylazine (5 mg/kg)) rabbits were injected intravenously with heparin (2500 IU) and were sacrificed by a percussive blow to the head. SHAM-operated animals served as controls. The rabbits did not show any confounding diseases.

2.2 Cardiac myocyte isolation

For isolation of AM, rabbits were sacrificed and hearts were rapidly extracted. Single cardiac myocytes from the left atrium were obtained by enzymatic dissociation through retrograde perfusion of the aorta. First, the water bath for the isolation system (± 37 °C) was turned on. Next, the two chambers of the system were filled out with Millipore water and were washed three times. Afterwards, solutions were prepared (Supplemental tables 1, 2 & 3). Solution A was placed in the big chamber while Solution Enzyme was placed in the small chamber. Subsequently, the heart was placed in cold Solution A and massaged gently. The heart was cannulated via the aorta, tied up to the cannula and washed with Solution A (from the big chamber) for about 8 minutes. Afterwards, the heart was perfused with Solution Enzyme for 15 minutes in total. The heart was cut into three pieces: the right atrium, the left atrium, and the left ventricle. Each piece was transferred to the corresponding beaker containing 20 mL Solution Storage. The tissue pieces were minced and subsequently filtered through a 200 µm nylon mesh. Next, Ca^{2+} was increased every 10 minutes up to a final concentration of 1000 µM by the following steps: 50 µM, 100 µM, 200 µM, 400 µM, 600 µM, 800 µM, 1000 µM. Finally, the number and the quality of the cells were checked under the microscope. The tubing of the system was washed with Millipore water, ethanol and dried.

2.3 Immunocytochemistry

Coverslips (Ø 13 mm, Thermo Scientific, Belgium) were coated with laminin solution (40 µl/ml) and incubated overnight at 4 °C. Laminin coated coverslips were placed in 35 mm plastic petri dishes to which left atrial cell suspension was added for 2 hours. Next, isolated rabbit AM were stained with Alexa Fluor 633-conjugated Wheat Germ Agglutinin (WGA) to visualize the membrane. Subsequently, AM were placed in a perfusion bath with pressure (0,8 psi) and temperature (37 °C) control. Cells were perfused for 5 minutes during field stimulation (1 Hz) with 1) normal Tyrode (NT; Supplemental table 4) solution for baseline or with 2) Isoproterenol (ISO; 300 nM; Supplemental table 5), a β-adrenergic agonist (32). After fixation with 2% paraformaldehyde (PFA), cells were permeabilized with 0.5% Triton X-100 in phosphate buffered saline (PBS) for 10 minutes and washed with PBS. Next, cells were blocked with 10% normal goat serum in PBS for 1 hour. Afterwards, cells were washed and incubated with primary antibody against RyR (1:50, mouse-anti-RyR C3-33, Thermo Fisher Scientific) overnight at 4 °C. Furthermore, secondary antibody (1:50, Alexa Fluor 488 labeled goat anti-mouse antibody, Abcam, Cambridge, UK) was used for 2 hours at room temperature (Supplemental figure 3). Labeling of anti-P2808-RyR with Zenon labeling kit (Alexa Fluor 532 rabbit IgG labeling kit, Thermo Fisher Scientific) was performed according to the manual. Next, cells were washed and fixated with 4% PFA. Afterwards, cells were washed once in PBS, embedded with mounting medium (Mowiol/DABCO) and covered with suitable coverslips. Confocal fluorescence images of AM after triple immunostainings were obtained with a LEICA TCS SPE and NIKON C1 on NIKON Eclipse TE-2000 inverted microscope. The pinhole was set at 1 airy unit (46/56 µm). Fluorophores were excited at 488 nm, 532 nm, and 633 nm and emission was detected at 500-532 nm, 544-633 nm, and 645-745 nm. Part of the freshly isolated cells were used to assess fluorescent Ca^{2+} measurements as described in the following section.

2.4 Calcium measurements

Ca^{2+} transients were recorded during field stimulation (1 Hz, 37 °C) (45) in rabbit AM loaded with fluo-4 acetoxymethyl ester. Transversal line-scan images of cytosolic Ca^{2+} signals were obtained by using confocal microscopy. During each experiment scanning speed, excitation, and amplification settings were kept constant. Fluorescence intensity values of line-scan images (F) were normalized to the fluorescence intensity values at rest (F0). Normalized fluorescence intensity ratios were plotted against time. Ca^{2+} measurements were performed and analyzed by Patrick Schönleitner.

2.5 ImageJ (Fiji)

2.5.1 RyR-P2808 signal analysis of RyR-clusters

The fraction of highly phosphorylated (P2808)-RyR clusters among all clusters was determined using ImageJ (Fiji). Normalized P2808-signals were calculated from confocal immunofluorescence images of approximately 100 x 100 nm pixel size. Regions of interest (ROIs) were selected from which nuclear signals were omitted as they reflect unspecific cross-reactions of the RyR-P2808 antibody. Cytosolic RyR-P2808, RyR and WGA signals were background-corrected by subtracting the modal grayscale value for each ROI. After local contrast enhancement (CLAHE) and image smoothing (3 x 3 mean filter), RyR clusters were detected within an approximate tolerance of 15 grayscale levels (8-bit grayscale image) (42). A binarized image was generated, dilated, and subjected to water shedding (42). The binarized image represented combined cluster detection from both channels (RyR and RyR-P2808). Next, the average normalized RyR-P2808 was calculated for each resulting cluster-segment as P2808/RyR ratio data (42). RyR-P2808 signals throughout a given cluster population were graphed as a frequency distribution histogram (bin size 0.2) (42). Experimental data were normalized by using the second peak position of the cluster phosphorylation distribution in the ISO population as threshold.

2.5.2 Proximity analysis of RyR-P2808 signals

A proximity analysis was carried out using ImageJ (Fiji) to determine spatial relations of RyR-clusters relative to the membrane. In analogy to the RyR-P2808 signal analysis of RyR-clusters described above, confocal immunofluorescence images of 100 nm pixel size were used. WGA signals were binarized by local Otsu-thresholding following local contrast enhancement and image smoothing (3x3 mean filter). Images were segmented into AT, UC and SS. Local positions of RyR-P2808 signals were determined as local signal maxima (at ± 15 grayscale levels noise tolerance) (42).

2.6 Statistical analysis

GraphPad Prism 5 (GraphPad Software, San Diego, CA, USA) and Microsoft Excel were used to perform statistical analyses. Results were tested for normality and subsequently compared by unpaired 2-tailed Student's t-test, Mann-Whitney U test, or ANOVA. When normality test (Shapiro-Wilk test) was fulfilled, a parametric test (t-test, ANOVA) was used. Where normality test failed, a non-parametric test (Mann-Whitney U-test) was used. A value of $p<0.05$ was considered as statistically significant.

2.7 Study approval

Animal handling was performed according to the European directive on laboratory animals 2010 / 63 / EU. The animal protocol was approved by the Local Ethical Committee for animal research at Maastricht University (DEC).

3 Results

3.1 B-adrenergic stimulation normalizes global Ca^{2+} transient amplitude in atrial RAP cells

In a first set of experiments, we compared the effect of β-adrenergic stimulation on global Ca^{2+} transients between SHAM and RAP. Figure 4 shows typical recordings of Ca^{2+} transients in field-stimulated myocytes from SHAM and RAP under baseline and after β-adrenergic stimulation. Ca^{2+} traces were averaged from transversal line scan images (Figure 4, lower panel). Under baseline, Ca^{2+} transient amplitude was significantly reduced in atrial RAP cells when compared with atrial SHAM cells (Figure 5). ISO increased the amplitude and accelerated the decline of the Ca^{2+} transient; these inotropic and lusitropic effects of β-adrenergic stimulation on Ca^{2+} were observed in both SHAM and RAP. Interestingly, the relative response to β-adrenergic stimulation was larger in RAP. Ca^{2+} transient amplitude, time to peak (TTP) and Ca^{2+} transient decline were normalized to SHAM levels after β-adrenergic stimulation. Averaged data are shown in Figure 5.

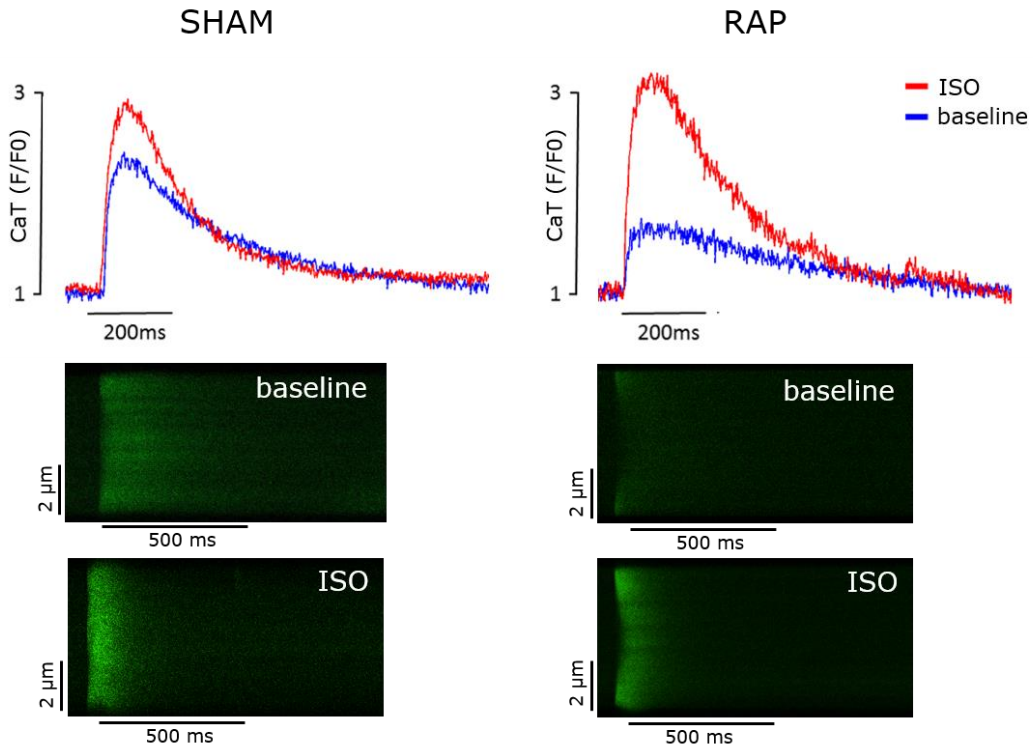

Figure 4 Representative recordings of global Ca^{2+} transients. *Ca^{2+} transients (CaT) were recorded in an atrial myocyte from a SHAM-operated rabbit (left) and a RAP rabbit (right) at baseline (normal Tyrode; NT, blue) and after β-adrenergic stimulation (Isoproterenol; ISO, 300 nM, red). Global Ca^{2+} transients are averaged fluo-4 signals from transversal confocal line scans. F indicates fluorescence intensity and F0 indicates fluorescence intensity at rest. Normalized fluorescence was plotted against time. Scale bars: 2 µm.*

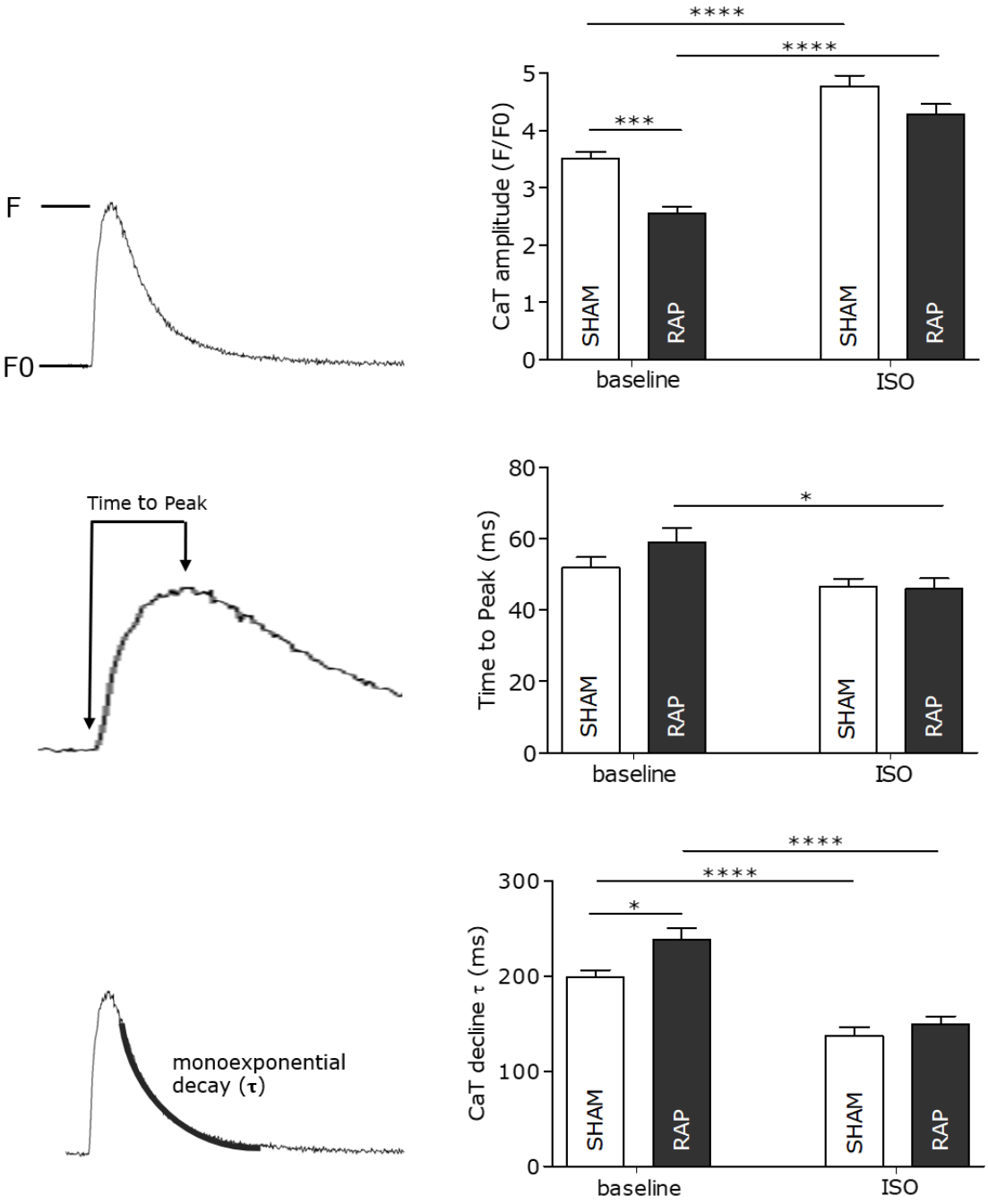

Figure 5 Effect of β-adrenergic stimulation on global Ca^{2+} transients. *Left: Analysis of Ca^{2+} transient (CaT) amplitude and kinetic parameters, time to peak (TTP) and Ca^{2+} transient decline (tau). Right: pooled data of five SHAM (baseline, n= 72 cells; ISO, n= 57 cells) and five RAP (baseline, n=34 cells; ISO, n= 43 cells) rabbits. Ca^{2+} transient amplitude was expressed as F (fluorescence intensity) divided by F0 (fluorescence intensity at rest). * denotes p<0,05. *** denotes p<0,001. **** denotes p<0,0001.*

3.2 B-adrenergic stimulation recruits RyR-clusters in atrial RAP cells

Next, we investigated at the structural level the phosphorylation of RyR clusters. PKA-dependent RyR-phosphorylation was assessed by immunostainings of RyR (green) and PKA-phosphorylated RyR-P2808 (red). Merged signals (yellow) indicate phosphorylation of RyR clusters. In the example of a co-labeled SHAM myocyte (Figure 6A), RyR clusters show a regular striated pattern, and phosphorylation was observed at baseline and after ISO. In RAP, phosphorylation levels were very low under baseline but increased after ISO (Figure 6A). To quantify changes in PKA-dependent RyR-phosphorylation in response to ISO, RyR clusters were identified in individual myocytes, and for each cluster, the normalized P2808/RyR signal was calculated. The P2808/RyR values of the cluster population were then plotted as a frequency distribution. The peak of the histogram represents the highest frequency (y-axis) of a given P2808/RyR ratio (x-axis). A leftward shift of the peak indicates less phosphorylation, and vice versa, the more the peak is shifted to the right on the x-axis, the more phosphorylation of RyR at serine 2808 is present. Figure 6B compares histograms for RyR cluster populations of untreated cells, and cells treated with ISO. To compare relative changes, frequency distributions were normalized to the peak position (i.e. interval on the x-axis with the highest frequency on the y-axis) of the ISO cluster population. The peak in SHAM was centered around bin 0.6 on the x-axis at baseline and shifted to the right after ISO, indicating a significant increase of baseline phosphorylation of RyR in response to ISO (Figure 6B). In RAP, no bimodal distribution was seen, suggesting RyR hypophosphorylation under baseline (maximal frequency at bin 0.2 on the x-axis). With ISO, a peak of high RyR phosphorylation appeared (Figure 6B). Taken together, our data indicate that 1) RyR is hypophosphorylated in RAP under baseline, and subsequently 2) the population of unphosphorylated RyR-clusters recruited by β-adrenergic stimulation is larger in RAP.

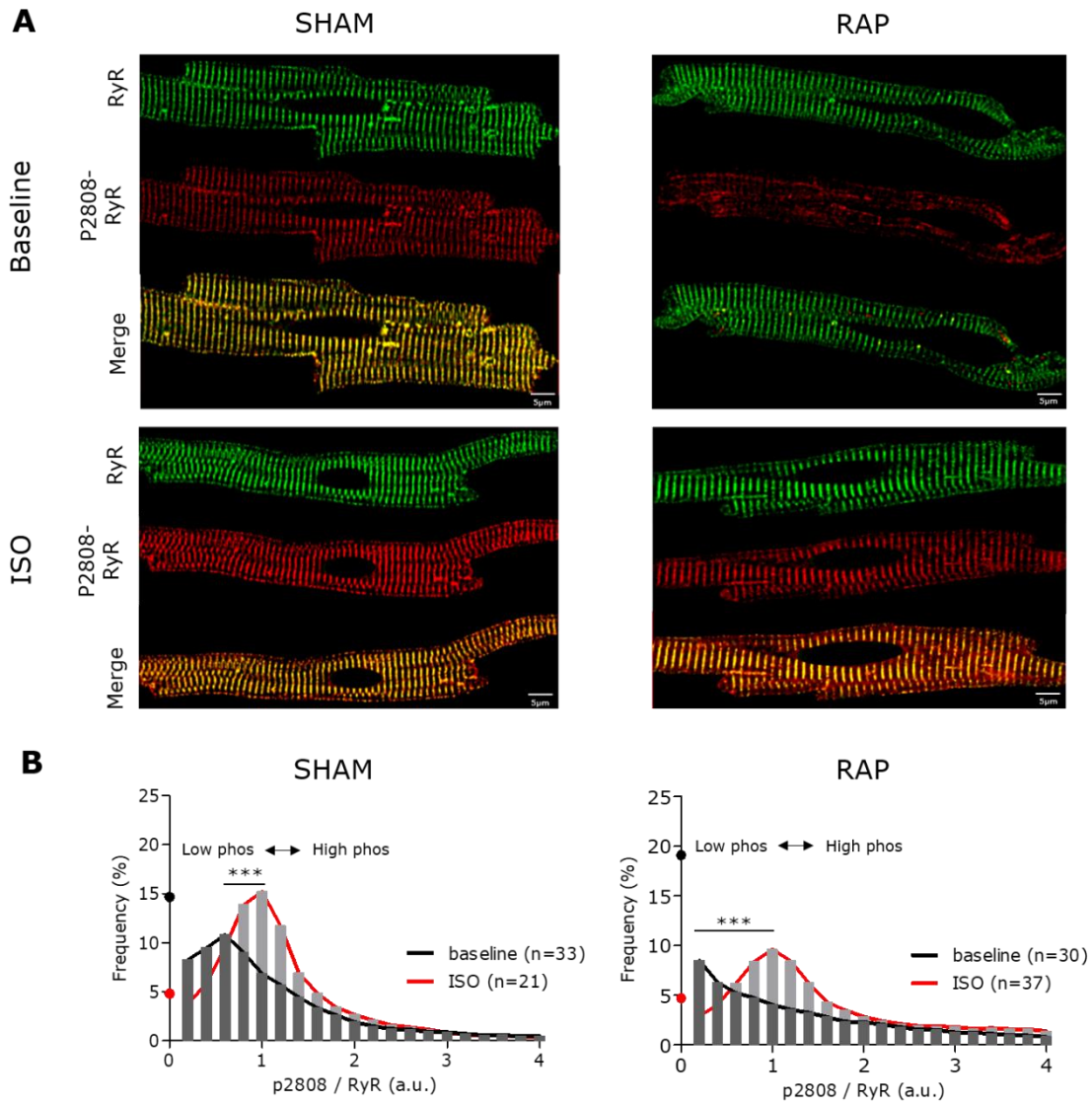

Figure 6 Effect of β-adrenergic stimulation on PKA-dependent RyR-phosphorylation. ***A,*** *Representative confocal images of RyR- and P2808-RyR-coimmunostained rabbit AM. Legend: RyR (green), P2808-RyR (red) and merge (overlay of RyR and P2808-RyR; yellow). Scale bars: 5 µm.* ***B,*** *Histograms showing frequency distribution of P2808/RyR normalized cluster signals in AM of four SHAM-operated and five RAP rabbits at baseline (NT) and after β-adrenergic stimulation (ISO). Zero bin values were represented as separate black and red data points. Black dots indicate baseline condition. Red dots indicate ISO condition. *** denotes p<0,0001.*

3.3 Differences of membrane-specific RYR-cluster phosphorylation between SHAM and RAP

The study by Brandenburg *et al.* identified distinct populations of low and highly phosphorylated RyR clusters in AM from mice, with sites of high phosphorylation preferentially located at TAT (42). Rodents typically have a more developed TAT network than larger animals (46). To confirm in rabbit AM the findings previously obtained in mice, we performed a frequency distribution analysis of phosphorylated RyR clusters in relation to the nearest membrane. Spatial relations of RyR-clusters relative to the membrane were investigated by performing triple immunostainings (RyR, P2808-RyR, WGA) (Figure 7A, C). In the first step, we applied a cluster analysis of a P2808/RyR image (Figure 7B) as described in the previous paragraph. Next, individual clusters were assigned to the nearest membrane structure identified by WGA staining: subsarcolemmal (SS, grey clusters) or AT (black clusters) (Figure 7C, D). Typically in AM, the majority of clusters is uncoupled (UC, red symbols) (Figure 7D). Frequency distribution analysis of the three subpopulations revealed that in SHAM cells, a peak of low phosphorylation could be detected for RyR clusters located at UC regions compared with higher phosphorylation of RyR clusters at coupled regions (i.e. AT and SS) (Figure 7E). As expected by the data of total RyR phosphorylation (Figure 6), there was no baseline RyR-phosphorylation present in AM isolated from RAP rabbits (Figure 7E).

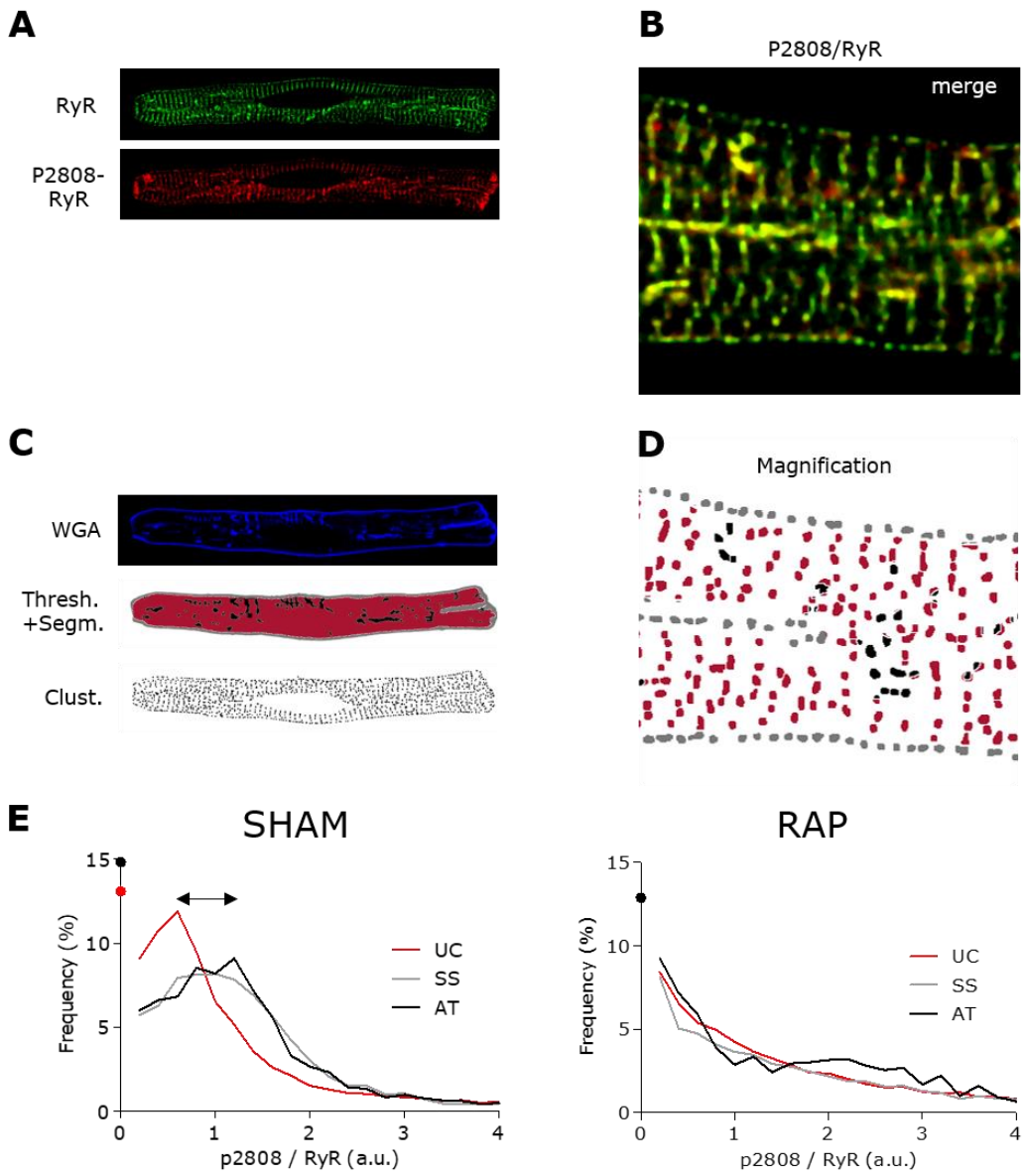

Figure 7 Differences of membrane-specific RyR-cluster phosphorylation between SHAM and RAP. A, *Confocal image of RyR staining (green) and P2808-RyR staining (red).* ***B,*** *Magnification (4x) of merged (i.e. overlay of RyR and P2808-RyR) images.* ***C,*** *Workflow of cluster analysis in relation to the nearest membrane. Legend: WGA (membrane staining), Thres.+Segm. (Thresholding and segmentation), Clust. (cluster identification).* ***D,*** *Magnification (4x) of RyR clusters. Color legend: grey dots indicate SS clusters, red dots indicate UC clusters, and black dots indicate AT clusters.* ***E,*** *Frequency histograms of the P2808/RyR cluster distribution at uncoupled (UC), subsarcolemmal (SS) and axial tubule (AT)-release sites in four SHAM (n= 33 cells) and five RAP (n= 30 cells) rabbits at baseline (NT). Arrow indicates shift on the x-axis in phosphorylation (UC vs. SS and AT). Zero bin values were not included in the graphs but were represented as separate data points. Black dots indicate AT zero bin values. Red dot indicates UC zero bin value.*

3.4 Divergent β-adrenergic regulation of RyR-cluster phosphorylation in SHAM *versus* RAP

We further investigated whether microdomain-specific RyR-phosphorylation was altered in SHAM *versus* RAP after β-adrenergic stimulation (ISO). Triple immunostainings (RyR, P2808-RyR, WGA) were performed on AM isolated from four SHAM-operated rabbits and five RAP rabbits. A frequency distribution analysis of phosphorylated RyR clusters was performed in relation to the nearest membrane (Figure 8). As illustrated in Figure 7, baseline RyR-phosphorylation in SHAM cells appeared to be higher at AT and SS regions compared to UC regions. B-adrenergic stimulation shifted the frequency distributions to the right; this shift was most pronounced for RyR phosphorylation at the UC (Figure 8). In RAP cells, no baseline phosphorylation was observed (Figure 7). Interestingly, the β-adrenergic rescue of RyR-phosphorylation in RAP cells involved equal recruitment of RyR at UC, SS and AT regions (Figure 8).

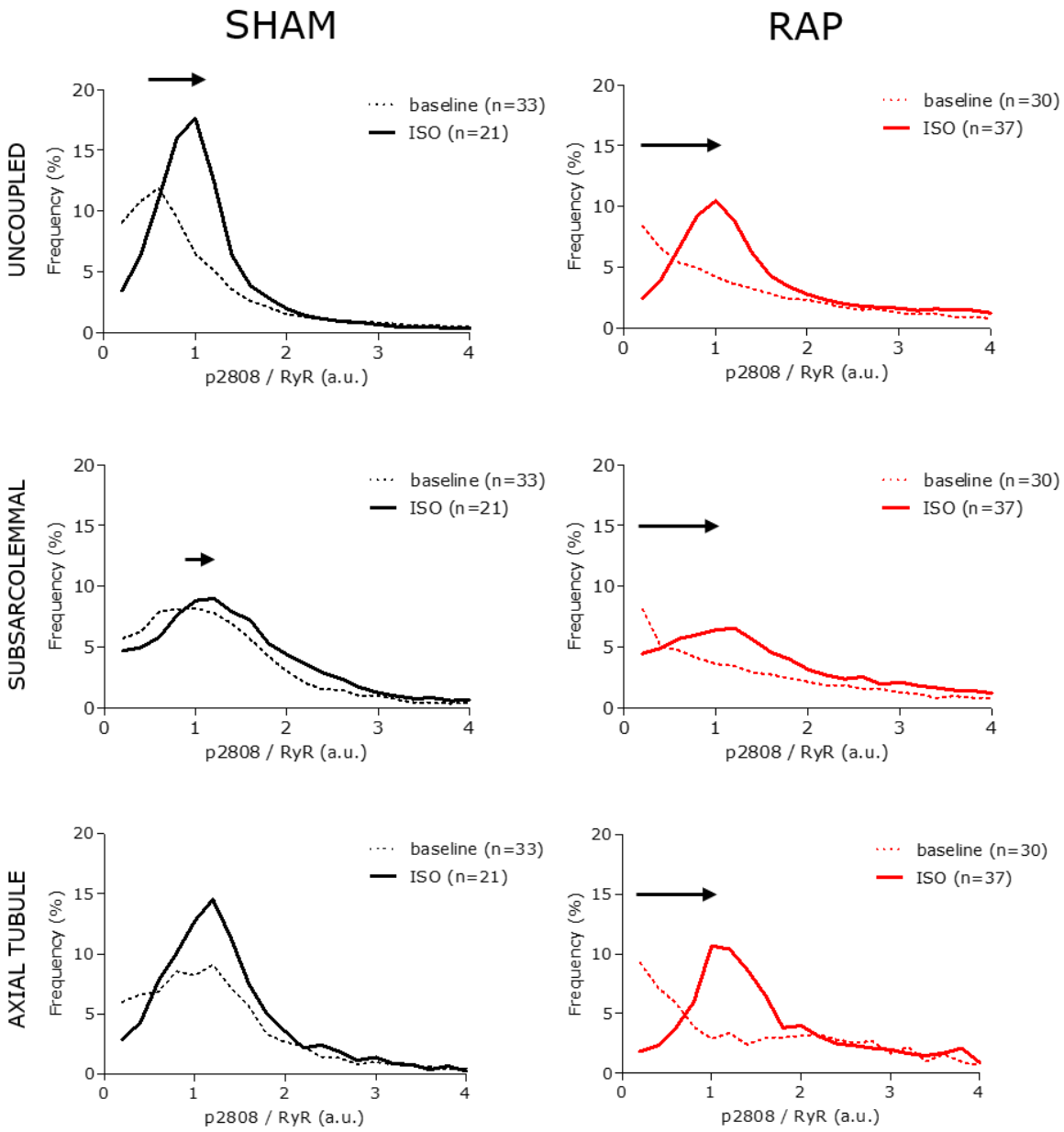

Figure 8 B-adrenergic regulation of RyR-cluster phosphorylation in SHAM versus RAP. *Frequency distribution histograms of P2808/RyR clusters at uncoupled (UC), subsarcolemmal (SS) and axial tubule (AT)-release sites in AM of four SHAM rabbits (left) and five RAP rabbits (right) at baseline (NT) and after β-adrenergic stimulation (ISO).*

3.5 Is microdomain-specific RyR phosphorylation correlated with faster Ca^{2+} release?

Finally, we correlated structural data of microdomain-specific in situ phosphorylation obtained in this thesis (i.e. triple immunostainings of RyR-phosphorylation) with functional data (i.e. measurements of Ca^{2+} transients) previously collected by Patrick Schönleitner (Figure 10). In rabbit AM, loaded with a Ca^{2+} dye and a membrane dye to visualize TAT, Ca^{2+} transients were imaged along a transversal line passing through an AT. Local Ca^{2+} transients were analyzed at axial tubules (AT), subsarcolemmal (SS), and cytosolic uncoupled regions (UC) (Figure 9). The left panel of Figure 10 shows pooled data of Figure 8 comparing SHAM and RAP for the three RyR subpopulations. The right panel shows TTP of Ca^{2+} transients at UC, AT and SS release sites (Figure 10). TTP is an indirect indication of the rate of Ca^{2+} release, and we expect faster release with increased RyR phosphorylation. On the global level, ISO decreased TTP (Figure 5), which is associated with an overall increase in RyR phosphorylation (Figure 6). In SHAM, the ISO-induced TTP decrease was most significant at the UC sites (Figure 10). This is consistent with our observation that ISO preferentially recruits UC RyR, that unlike AT and SS have low baseline phosphorylation levels (Figure 7E). In RAP, TTP is slowest at UC which is associated with RyR hypophosphorylation; compared to SHAM, the larger decrease in TTP by ISO correlates to a larger shift in RyR phosphorylation. To summarize, rapid atrial pacing causes RyR-hypophosphorylation in RAP that can be reversed by β-adrenergic stimulation. This correlates with the β-adrenergic shortening of TTP observed at UC sites in RAP.

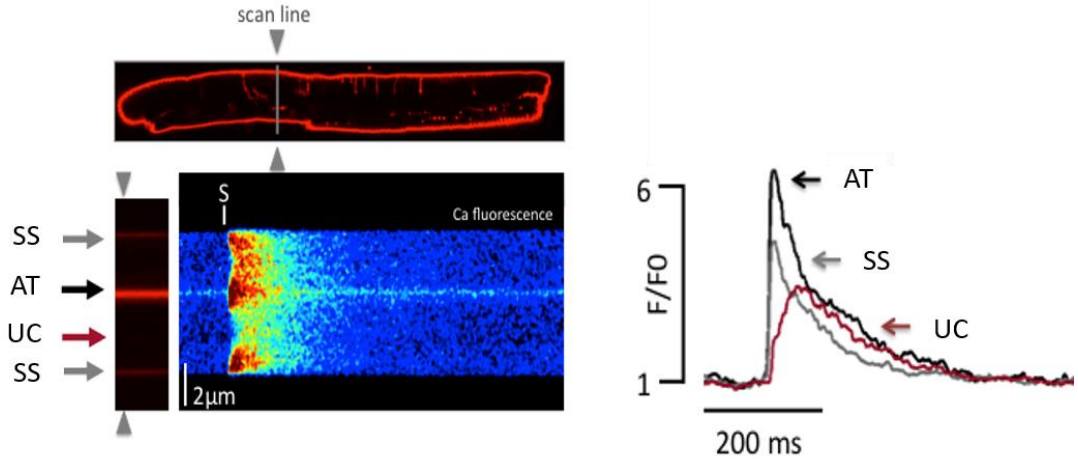

Figure 9 Local Ca^{2+} transient measurement setup. *Ca^{2+} transients were recorded during field stimulation (1 Hz, 37 °C) in rabbit AM. Transversal line-scan images of cytosolic Ca^{2+} signals were obtained at axial tubules (AT), subsarcolemmal (SS), and cytosolic uncoupled regions (UC) by using confocal microscopy. Normalized fluorescence intensity ratios (F/F0) were plotted against time. Scale bar: 2 µm.*

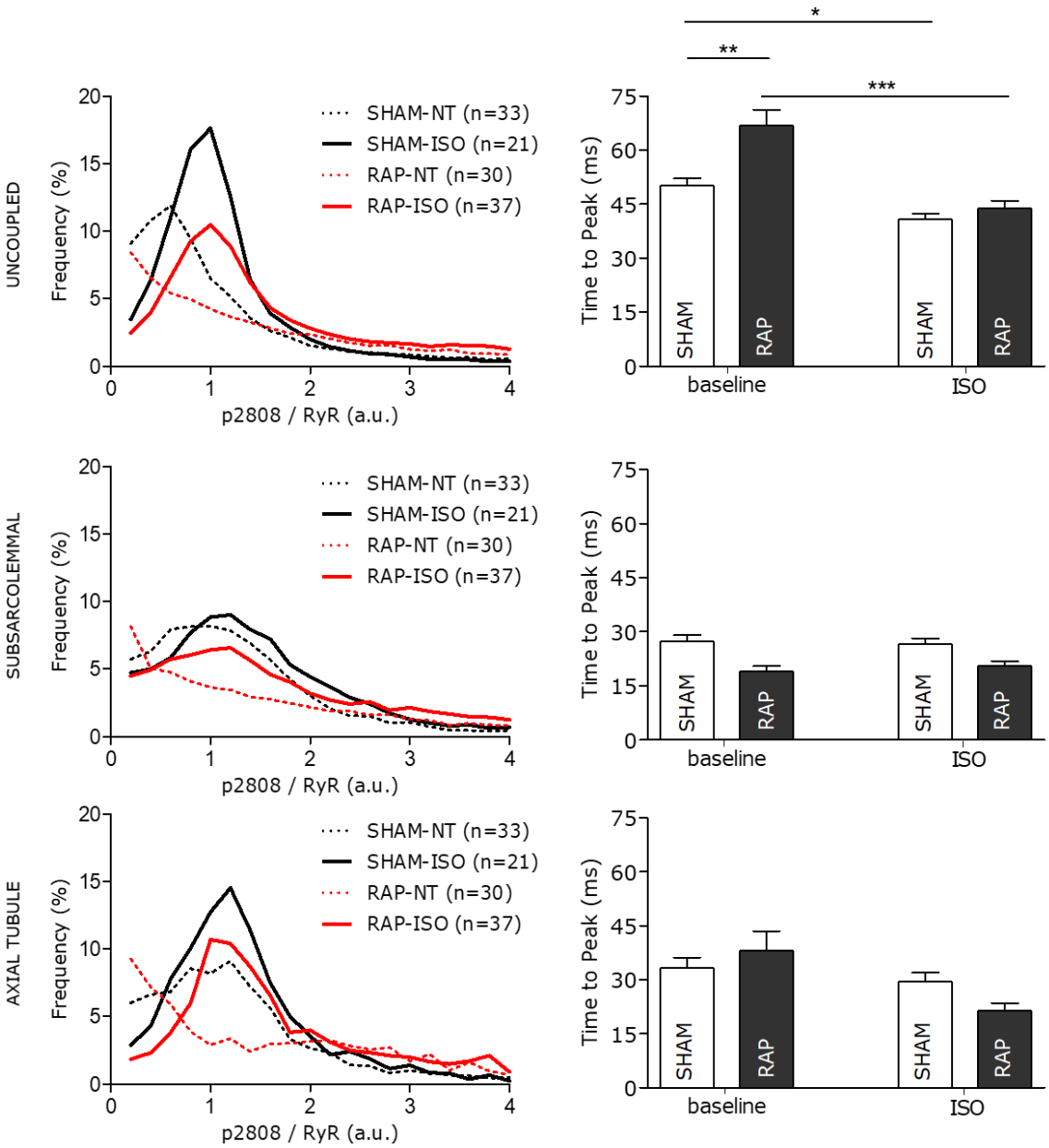

Figure 10 Correlation of microdomain-specific RyR phosphorylation with microdomain-specific Ca^{2+} release rate. *Left: Frequency histograms of the P2808/RyR cluster distribution at uncoupled (UC), subsarcolemmal (SS), and axial tubule (AT)-release sites in RAP and SHAM rabbits at baseline (NT) and after β-adrenergic stimulation (ISO). Right: TTP at UC, SS and AT regions in SHAM rabbit AM and RAP rabbit AM at baseline and after ISO. * denotes p<0,05. ** denotes p<0,001. *** denotes p<0,0001.*

4 Discussion

In a rabbit model of tachy-paced atrial remodeling, the amplitude of baseline Ca^{2+} transients is significantly reduced (Greiser et al. (32), Supplemental figure 4). In this study, we additionally showed in RAP rabbit cells that the Ca^{2+} transient amplitude significantly increased after β-adrenergic stimulation to a similar level as in SHAM cells. Similarly, global RyR-phosphorylation was significantly reduced in RAP cells at baseline but showed a greater relative increase after β-adrenergic stimulation. Subcellularly, baseline RyR-phosphorylation in SHAM cells appeared to be higher at AT and SS regions compared to UC regions. B-adrenergic stimulation shifted the frequency distributions to the right; this shift was most pronounced for RyR phosphorylation at the UC regions. In RAP cells at the subcellular level, the β-adrenergic rescue of RyR-phosphorylation involved equal recruitment of RyR at UC, SS and AT regions. In summary, rapid atrial pacing causes RyR-hypophosphorylation in RAP that can be reversed by β-adrenergic stimulation. This correlates with the β-adrenergic shortening of TTP observed at UC sites in RAP.

To unravel the underlying molecular mechanisms of AF, there is a necessity for a suitable animal model. A variety of animal models exist to study the pathophysiology of AF (47). However, none of these models completely reflect the human phenotype due to its complexity. Each of the existing animal models reproduces a specific component of the pathophysiology of clinical AF (47). For this project, a rabbit model of tachycardia-induced atrial remodeling was used (44). This model recapitulates some main features of human AF, including AP shortening and Ca^{2+} signaling disturbances (32-35). Rabbit hearts are more similar to human in terms of Ca^{2+} signaling than rodents. In rabbit myocytes, 70% of the Ca^{2+} is removed by SERCA (into the SR), while 28% leaves the cytosol through NCX, and 1% is removed by the sarcolemmal Ca^{2+}ATPase and mitochondrial Ca^{2+}uniporter (13). In rats, SERCA activity is higher and NCX Ca^{2+} removal is lower compared to rabbits. This results in a balance of 92% for SERCA, 7% for NCX and 1% for the sarcolemmal Ca^{2+}ATPase and mitochondrial Ca^{2+}uniporter to remove Ca^{2+} (13). In addition, it is known that rodents typically have a more developed TAT network than rabbits and humans (46). Thus, rabbits are a suitable model to study Ca^{2+} handling, and remodeling due to tachypacing.

4.1 B-adrenergic stimulation normalizes global Ca^{2+} transients and recruits RyR clusters in atrial RAP cells

First, we investigated the effect of β-adrenergic stimulation on global Ca^{2+} transients between SHAM and RAP by measuring Ca^{2+} transient amplitude, TTP, and Ca^{2+} transient decline. Under baseline, Ca^{2+} transient amplitude was significantly reduced in atrial RAP cells when compared with atrial SHAM cells. This finding confirmed the study of Greiser *et al.* (Supplemental figure 4) (32). ISO significantly increased the amplitude and accelerated the decline of the Ca^{2+} transient. Thus, β-adrenergic stimulation (i.e. ISO) exerted an inotropic and lusitropic effect on Ca^{2+} in both SHAM and RAP (13). A striking finding was that the relative response to β-adrenergic stimulation was larger in RAP cells, which can cause triggered activity. This rescue might suggest that β-adrenergic stimulation modifies Ca^{2+} signaling in RAP rabbits in a different way than in SHAM rabbits. There are some data on the rescue of the ICaL and the Ca^{2+} transient after β-adrenergic stimulation. Wagoner *et al.* (39) already demonstrated that ICaL was lower in myocytes from chronic AF patients and that the lowered ICaL was rescued in response to maximal β-adrenergic stimulation (Supplemental figure 2) (39). Voigt *et al.* (35) observed 50% and 48% lower amplitudes of ICaL and Ca^{2+} transient, respectively, in chronic AF patients when compared to controls. However, diastolic $[Ca^{2+}]i$ appeared to be higher in chronic AF patients than in controls. The higher diastolic $[Ca^{2+}]i$ was due to an enhanced SR Ca^{2+} leak through CaMKII-hyperphosphorylated RyR together with larger I_{NCX}, causing triggered activity (i.e. DAD and EAD) in chronic AF patients (35). To further understand the rescue in RAP cells, we examined Ca^{2+} release at the structural level. Structurally, many different proteins (e.g. LTCC, RyR) and post-translational modifications (e.g. phosphorylation, ROS-dependent modifications) could be involved. A study by Voigt *et al.* (36) showed that DAD occurrence in patients with paroxysmal AF has been associated with an excessive increase in SR Ca^{2+} load and increased RyR activity. The increased SR Ca^{2+} load was related to PKA-dependent PLB phosphorylation. The mechanisms by which RyR activity was increased, were unknown but were unrelated to CaMKII (36). Accordingly, we focused on the phosphorylation of RyR, which is known to play an important role in Ca^{2+} signaling and AF (11, 30, 48, 49). PKA is the most common downstream effector of β-adrenergic signaling (14, 16) and is responsible for RyR phosphorylation at serine 2808 (15, 17, 25, 50, 51). Therefore, triple immunostainings were carried out on AM to observe global PKA-dependent RyR-phosphorylation. Baseline phosphorylation of RyR significantly increased in response to ISO in SHAM rabbits. RyR were hypophosphorylated in RAP under baseline. However, the recruitment of unphosphorylated RyR clusters after β-adrenergic stimulation was larger in RAP.

4.2 Microdomain specific β-adrenergic regulation of RyR cluster phosphorylation is divergent in SHAM *versus* RAP

As less is known about PKA-dependent modulation of RyR at microdomain level, we developed a method for analyzing microdomain-specific RyR phosphorylation by assigning phosphorylated clusters to the nearest membrane. A WGA staining was used to visualize the membrane and was combined with a cluster analysis (as described in (42)) to identify RyR located at SS, UC and AT. We then investigated whether microdomain-specific RyR-phosphorylation was altered in SHAM *versus* RAP at baseline and after β-adrenergic stimulation. Baseline RyR-phosphorylation in SHAM cells was higher at AT and SS compared to UC regions. B-adrenergic stimulation shifted the frequency distributions to the right with a shift most pronounced for RyR phosphorylation at the UC. As RyR at UC regions were less phosphorylated at baseline, they are recruited more likely after β-adrenergic stimulation. B-adrenergic rescue of RyR-phosphorylation in RAP cells involved equal recruitment of RyR at UC, SS and AT regions. Findings of the current study were in line with findings of similar studies. A study by Brandenburg *et al.* (42) in healthy mice AM demonstrated that the rate of Ca^{2+} release is slower at UC regions. In these regions, RyR are activated through propagated Ca^{2+} release with a delay due to the absence of TAT; low baseline RyR-phosphorylation lowering RyR Ca^{2+} sensitivity may further slow Ca^{2+} propagation at the UC. The Brandenburg study (42) in healthy mice AM identified microdomains of low and highly phosphorylated RyR clusters with sites of high phosphorylation preferentially located at AT (42). We confirmed this finding of high baseline RyR phosphorylation at AT regions in SHAM rabbits (13, 46). Furthermore, recent evidence suggested that the regulation of RyR release sites by kinases (CaMKII, PKA) is selective for coupled and uncoupled RyR Ca^{2+} microdomains (19, 41, 42). A study by Dries *et al.* (19) already investigated CaMKII-dependent modulation of RyR activity. In this study (Dries *et al.* (19)), they showed that CaMKII-dependent modulation of RyR was restricted to coupled RyR in the dyadic cleft (41). In line with these findings, our data suggest that the level of PKA-dependent RyR phosphorylation depends on the subcellular location in AM.

4.3 Are microdomain-specific highly phosphorylated RyR clusters correlated with a faster Ca^{2+} release?

In cardiac myocytes, the generation and diffusion of Ca^{2+} signals is limited in time and space in Ca^{2+} microdomains (40). Subcellularly, RyR-mediated Ca^{2+} release is known to be heterogeneous with sites of slow release (uncoupled RyR) and fast release (RyR near axial membranes (TAT) and sarcolemma) (42, 43). We, therefore, investigated next whether the level of RyR phosphorylation correlated with the rate of Ca^{2+} release. To investigate this, TTP was measured at UC, SS and AT, and correlated with structural data of microdomain-specific RyR phosphorylation. TTP is an indirect indication of the rate of Ca^{2+} release, and we expect faster release with increased RyR phosphorylation. As previously mentioned, ISO decreased TTP at the global level. This is associated with an overall increase in RyR phosphorylation in RAP cells. In SHAM cells, ISO-induced TTP decrease was most significant at the UC sites. This observation is consistent with the preference of UC RyR recruitment by ISO. In RAP, TTP is slowest at UC which is associated with RyR hypophosphorylation. The larger decrease in TTP by ISO in RAP cells compared to SHAM cells correlates with a larger shift in RyR phosphorylation. To summarize, rapid atrial pacing causes RyR-hypophosphorylation in RAP that can be reversed by β-adrenergic stimulation. This correlates with the β-adrenergic shortening of TTP observed at UC sites in RAP. It should, however, be noted that TTP is an indirect measure of the Ca^{2+} release rate, and is therefore not directly linked to RyR phosphorylation.

4.4 Limitations

In this study, we wanted to investigate the association between PKA-dependent RyR phosphorylation and Ca^{2+} transients (i.e. microdomain-specific Ca^{2+} release). Therefore, we measured Ca^{2+} transients and used TTP as an indirect measure of the Ca^{2+} release rate. This indirect measure could form a potential limitation of the present study. Ca^{2+} transients depend on a variety of factors including the size of the ICaL, the SR content, and the state of the RyR. As we report that the Ca^{2+} transient, more specifically the TTP, is directly linked to RyR, we exclude the effect of the ICaL and the SR content.

A second limitation of the present study is that only UC, SS and AT domains were possible to include, as no discrimination could be made with the cluster analysis between TT and AT.

A third limitation is that also other mediators regulate Ca^{2+} handling, such as CaMKII. However, there is controversy about its activation. It is not clear whether CaMKII activation occurs via EPac and NOS1 (Pereira *et al*. (20); Supplemental figure 1) or via NOS1 without EPac (Dries *et al.* (19)). Nevertheless, both studies suggested that there is no effect of PKA on Ca^{2+} handling but that the effect on Ca^{2+} handling is all due to CaMKII. This thought has been questioned and the exact mechanisms behind PKA regulation of RyR remain controversial. A study by Bers *et al.* (25) suggested that phosphorylation of serine 2808 was relatively insensitive to PKA. In addition, another study suggested that PKA does not have a significant effect on RyR sensitivity in ventricular cardiac myocytes (41). The latter study investigated this by measuring Ca^{2+} sparks (i.e. indicator for SR content and RyR activity). PKA increased the SR Ca^{2+} content and the Ca^{2+} transient amplitude and so generated more Ca^{2+} sparks. However, after normalization, no significant effect of PKA on RyR was observed. In contrast, Wehrens *et al.* (50) provided evidence that PKA phosphorylation of serine 2808 on RyR is a critical mediator of progressive cardiac dysfunction.

Finally, each existing animal model only partly reflects the complex AF human phenotype. Because of this, clinical trials are needed before translating findings towards the clinic.

5 Conclusion and outlook

In conclusion, our study shows that the level of PKA-dependent RyR phosphorylation depends on the subcellular location in AM. Atrial remodeling due to rapid pacing causes RyR-hypophosphorylation that can be reversed by β-adrenergic stimulation. This mechanism could, at least partly, contribute to the β-adrenergic rescue of Ca^{2+} transients in AF improving contractility, but could adversely increase the likelihood of arrhythmias.

In the future, additional experiments could be carried out. As the Ca^{2+} transient not only depends on RyR activity but also depends on the LTCC and the SR Ca^{2+} loading, we could investigate the rescue of the latter two. Secondly, we could examine RyR activity more directly. This can be done by the investigation of Ca^{2+} sparks. Next, it is important to know what signalosomes are involved in the microdomain-specific regulation of RyR. We could investigate this to understand the baseline phosphorylation observed in normal rabbits. The reduced baseline phosphorylation of RyR at UC regions may, for example, be due to phosphodiesterases. Finally, we could investigate other microdomain-specific modulators of RyR (e.g. CaMKII) in AF. Thus, a lot of challenging work lies ahead to further improve our understanding in the underlying molecular mechanisms of AF.

6 Valorisation

AF is the most common cardiac arrhythmia, affecting 2% of the general population. The number of people with AF is estimated to more than double in the next fifty years, due to aging of the population (52). AF is associated with high morbidity and mortality that is predominantly mediated by ischemic stroke, myocardial infarction and the progression of HF. Because of this, it requires substantial societal and healthcare cost burdens. Despite its clinical importance, underlying mechanisms of AF are poorly understood. Better understanding of the underlying pathophysiology would be beneficial for AF treatment. This would lead to reduced therapy costs and higher life expectancy. To our knowledge, this study is the first to examine the effect of β-adrenergic regulation of microdomain-specific RyR phosphorylation in a tachycardia-induced rabbit model of atrial remodeling. This fundamental research is of great importance for the scientific community to better understand the mechanisms of microdomain signaling in AF, and brings us one step closer to unravel this complex disease. Therefore, our main audience would be the academic community or researchers in the field. The mechanism that was investigated plays an important role in AF and is an integral part of structural and functional remodeling. We revealed that the level of PKA-dependent RyR phosphorylation is microdomain-specific in AM. Tachycardia-induced atrial remodeling caused RyR hypophosphorylation that was reversed by β-adrenergic stimulation. On the one hand, this mechanism can contribute to the β-adrenergic rescue of Ca^{2+} transients in AF improving contractility. On the other hand, it can increase the likelihood of arrhythmias. This new knowledge could be helpful in the development of new (microdomain-specific) therapeutic approaches, adding value for society.

7 References

1.Fuster V, Ryden LE, Cannom DS, Crijns HJ, Curtis AB, Ellenbogen KA, et al. 2011 ACCF/AHA/HRS focused updates incorporated into the ACC/AHA/ESC 2006 guidelines for the management of patients with atrial fibrillation: a report of the American College of Cardiology Foundation/American Heart Association Task Force on practice guidelines. Circulation. 2011;123(10):e269-367.

2.Wyndham CR. Atrial fibrillation: the most common arrhythmia. Tex Heart Inst J. 2000;27(3):257-67.

3.Jansen HJ, Moghtadaei M, Mackasey M, Rafferty SA, Bogachev O, Sapp JL, et al. Atrial structure, function and arrhythmogenesis in aged and frail mice. Sci Rep. 2017;7:44336.

4.Heijman J, Voigt N, Nattel S, Dobrev D. Cellular and molecular electrophysiology of atrial fibrillation initiation, maintenance, and progression. Circ Res. 2014;114(9):1483-99.

5.January CT, Wann LS, Alpert JS, Calkins H, Cigarroa JE, Cleveland JC, Jr., et al. 2014 AHA/ACC/HRS guideline for the management of patients with atrial fibrillation: a report of the American College of Cardiology/American Heart Association Task Force on practice guidelines and the Heart Rhythm Society. Circulation. 2014;130(23):e199-267.

6.Markides V, Schilling RJ. Atrial fibrillation: classification, pathophysiology, mechanisms and drug treatment. Heart. 2003;89(8):939-43.

7.Allessie MA. Atrial electrophysiologic remodeling: another vicious circle? J Cardiovasc Electrophysiol. 1998;9(12):1378-93.

8.Wijffels MC, Kirchhof CJ, Dorland R, Allessie MA. Atrial fibrillation begets atrial fibrillation. A study in awake chronically instrumented goats. Circulation. 1995;92(7):1954-68.

9.Andrade J, Khairy P, Dobrev D, Nattel S. The clinical profile and pathophysiology of atrial fibrillation: relationships among clinical features, epidemiology, and mechanisms. Circ Res. 2014;114(9):1453-68.

10.Shen MJ, Zipes DP. Role of the autonomic nervous system in modulating cardiac arrhythmias. Circ Res. 2014;114(6):1004-21.

11.Vest JA, Wehrens XH, Reiken SR, Lehnart SE, Dobrev D, Chandra P, et al. Defective cardiac ryanodine receptor regulation during atrial fibrillation. Circulation. 2005;111(16):2025-32.

12.National Heart LaBI. How the Heart Works. 2017.

13.Bers DM. Cardiac excitation-contraction coupling. Nature. 2002;415(6868):198-205.

14.Ullrich ND, Valdivia HH, Niggli E. PKA phosphorylation of cardiac ryanodine receptor modulates SR luminal Ca2+ sensitivity. J Mol Cell Cardiol. 2012;53(1):33-42.

15.Marx SO, Reiken S, Hisamatsu Y, Jayaraman T, Burkhoff D, Rosemblit N, et al. PKA phosphorylation dissociates FKBP12.6 from the calcium release channel (ryanodine receptor): defective regulation in failing hearts. Cell. 2000;101(4):365-76.

16.Grimm M, Brown JH. Beta-adrenergic receptor signaling in the heart: role of CaMKII. J Mol Cell Cardiol. 2010;48(2):322-30.

17.Wehrens XH, Marks AR. Altered function and regulation of cardiac ryanodine receptors in cardiac disease. Trends Biochem Sci. 2003;28(12):671-8.

18.Takasago T, Imagawa T, Furukawa K, Ogurusu T, Shigekawa M. Regulation of the cardiac ryanodine receptor by protein kinase-dependent phosphorylation. J Biochem. 1991;109(1):163-70.

19.Dries E, Santiago DJ, Johnson DM, Gilbert G, Holemans P, Korte SM, et al. Calcium/calmodulin-dependent kinase II and nitric oxide synthase 1-dependent modulation of ryanodine receptors during beta-adrenergic stimulation is restricted to the dyadic cleft. J Physiol. 2016;594(20):5923-39.

20.Pereira L, Bare DJ, Galice S, Shannon TR, Bers DM. beta-Adrenergic induced SR Ca(2+) leak is mediated by an Epac-NOS pathway. J Mol Cell Cardiol. 2017;108:8-16.

21.Curran J, Tang L, Roof SR, Velmurugan S, Millard A, Shonts S, et al. Nitric oxide-dependent activation of CaMKII increases diastolic sarcoplasmic reticulum calcium release in cardiac myocytes in response to adrenergic stimulation. PLoS One. 2014;9(2):e87495.

22.Niggli E, Ullrich ND, Gutierrez D, Kyrychenko S, Polakova E, Shirokova N. Posttranslational modifications of cardiac ryanodine receptors: Ca(2+) signaling and EC-coupling. Biochim Biophys Acta. 2013;1833(4):866-75.

23.Mustroph J, Neef S, Maier LS. CaMKII as a target for arrhythmia suppression. Pharmacol Ther. 2017;176:22-31.

24.Cheng H, Lederer WJ, Cannell MB. Calcium sparks: elementary events underlying excitation-contraction coupling in heart muscle. Science. 1993;262(5134):740-4.

25.Bers DM. Cardiac ryanodine receptor phosphorylation: target sites and functional consequences. Biochem J. 2006;396(1):e1-3.

26.Valdivia HH. Ryanodine receptor phosphorylation and heart failure: phasing out S2808 and "criminalizing" S2814. Circ Res. 2012;110(11):1398-402.

27.Pereira L, Cheng H, Lao DH, Na L, van Oort RJ, Brown JH, et al. Epac2 mediates cardiac beta1-adrenergic-dependent sarcoplasmic reticulum Ca2+ leak and arrhythmia. Circulation. 2013;127(8):913-22.

28.January CT, Riddle JM. Early afterdepolarizations: mechanism of induction and block. A role for L-type Ca2+ current. Circ Res. 1989;64(5):977-90.

29.Xie Y, Liao Z, Grandi E, Shiferaw Y, Bers DM. Slow [Na]i Changes and Positive Feedback Between Membrane Potential and [Ca]i Underlie Intermittent Early Afterdepolarizations and Arrhythmias. Circ Arrhythm Electrophysiol. 2015;8(6):1472-80.

30.Li N, Chiang DY, Wang S, Wang Q, Sun L, Voigt N, et al. Ryanodine receptor-mediated calcium leak drives progressive development of an atrial fibrillation substrate in a transgenic mouse model. Circulation. 2014;129(12):1276-85.

31.Ihor Gussak CA, Arthur A.M. Wilde, Brian D. Powell, Michael J. Ackerman, Win-Kuang Shen. Electrical diseases of the heart. Springer.1.

32.Greiser M, Kerfant BG, Williams GS, Voigt N, Harks E, Dibb KM, et al. Tachycardia-induced silencing of subcellular Ca2+ signaling in atrial myocytes. J Clin Invest. 2014;124(11):4759-72.

33.Role of abnormal sarcoplasmic reticulum function in atrial fibrillation. Therapy. 2010;7(2):147-58.

34.Gomez-Hurtado N, Knollmann BC. Calcium in atrial fibrillation - pulling the trigger or not? J Clin Invest. 2014;124(11):4684-6.

35.Voigt N, Li N, Wang Q, Wang W, Trafford AW, Abu-Taha I, et al. Enhanced sarcoplasmic reticulum Ca2+ leak and increased Na+-Ca2+ exchanger function underlie delayed afterdepolarizations in patients with chronic atrial fibrillation. Circulation. 2012;125(17):2059-70.

36.Voigt N, Heijman J, Wang Q, Chiang DY, Li N, Karck M, et al. Cellular and molecular mechanisms of atrial arrhythmogenesis in patients with paroxysmal atrial fibrillation. Circulation. 2014;129(2):145-56.

37.Oral H, Crawford T, Frederick M, Gadeela N, Wimmer A, Dey S, et al. Inducibility of paroxysmal atrial fibrillation by isoproterenol and its relation to the mode of onset of atrial fibrillation. J Cardiovasc Electrophysiol. 2008;19(5):466-70.

38.Burashnikov A, Antzelevitch C. Late-phase 3 EAD. A unique mechanism contributing to initiation of atrial fibrillation. Pacing Clin Electrophysiol. 2006;29(3):290-5.

39.Van Wagoner DR, Pond AL, Lamorgese M, Rossie SS, McCarthy PM, Nerbonne JM. Atrial L-type Ca2+ currents and human atrial fibrillation. Circ Res. 1999;85(5):428-36.

40.Berridge MJ. Calcium microdomains: organization and function. Cell Calcium. 2006;40(5-6):405-12.

41.Dries E, Bito V, Lenaerts I, Antoons G, Sipido KR, Macquaide N. Selective modulation of coupled ryanodine receptors during microdomain activation of calcium/calmodulin-dependent kinase II in the dyadic cleft. Circ Res. 2013;113(11):1242-52.

42.Brandenburg S, Kohl T, Williams GS, Gusev K, Wagner E, Rog-Zielinska EA, et al. Axial tubule junctions control rapid calcium signaling in atria. J Clin Invest. 2016;126(10):3999-4015.

43.Trafford AW, Diaz ME, O'Neill SC, Eisner DA. Comparison of subsarcolemmal and bulk calcium concentration during spontaneous calcium release in rat ventricular myocytes. J Physiol. 1995;488 (Pt 3):577-86.

44.Milani-Nejad N, Janssen PM. Small and large animal models in cardiac contraction research: advantages and disadvantages. Pharmacol Ther. 2014;141(3):235-49.

45.Hamill OP, Marty A, Neher E, Sakmann B, Sigworth FJ. Improved patch-clamp techniques for high-resolution current recording from cells and cell-free membrane patches. Pflugers Arch. 1981;391(2):85-100.

46.Douglas P. Zipes JJ, William Gregory Stevenson. Cardiac Electrophysiology: From Cell to Bedside E-Book. 2017:1120

47.Nishida K, Michael G, Dobrev D, Nattel S. Animal models for atrial fibrillation: clinical insights and scientific opportunities. Europace. 2010;12(2):160-72.

48.Macquaide N, Tuan HT, Hotta J, Sempels W, Lenaerts I, Holemans P, et al. Ryanodine receptor cluster fragmentation and redistribution in persistent atrial fibrillation enhance calcium release. Cardiovasc Res. 2015;108(3):387-98.

49.Dobrev D, Voigt N, Wehrens XH. The ryanodine receptor channel as a molecular motif in atrial fibrillation: pathophysiological and therapeutic implications. Cardiovasc Res. 2011;89(4):734-43.

50.Wehrens XH, Lehnart SE, Reiken S, Vest JA, Wronska A, Marks AR. Ryanodine receptor/calcium release channel PKA phosphorylation: a critical mediator of heart failure progression. Proc Natl Acad Sci U S A. 2006;103(3):511-8.

51.Shan J, Kushnir A, Betzenhauser MJ, Reiken S, Li J, Lehnart SE, et al. Phosphorylation of the ryanodine receptor mediates the cardiac fight or flight response in mice. J Clin Invest. 2010;120(12):4388-98.

52.Zoni-Berisso M, Lercari F, Carazza T, Domenicucci S. Epidemiology of atrial fibrillation: European perspective. Clin Epidemiol. 2014;6:213-20.

8 Supplemental information

8.1 Supplemental figures

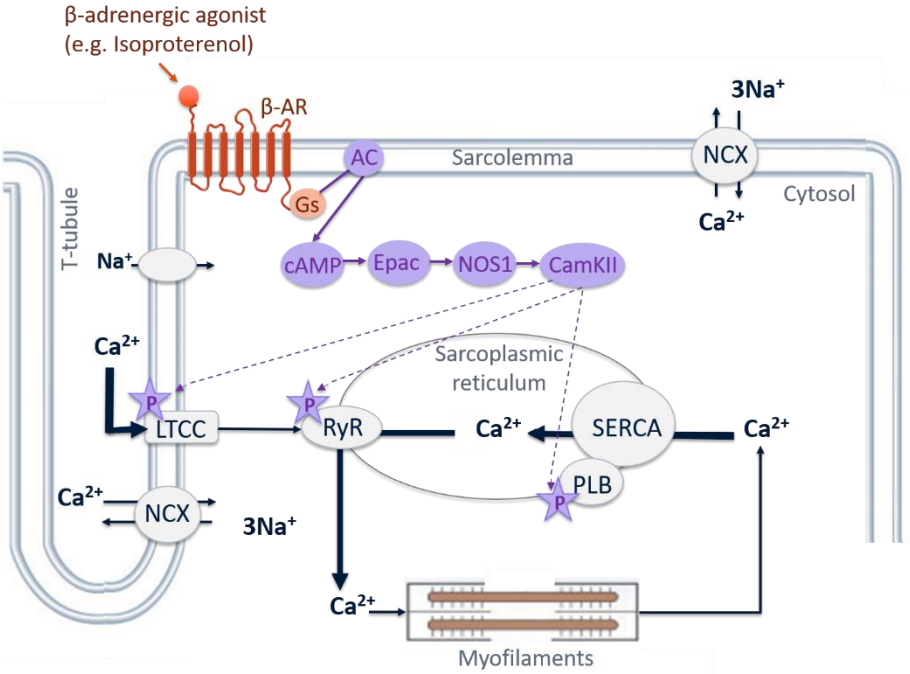

Supplemental figure 1 Calcium signaling after CaMKII-dependent β-adrenergic stimulation. *B-adrenergic agonist bind to β-adrenoreceptor (β-AR) stimulating G-protein (Gs) dependent activation of adenylyl cyclase (AC). This will cause cAMP production and subsequently activation of CaMKII which will phosphorylate its targets (i.e. LTCC, RyR and PLB). Asterisks with P indicate CaMKII-dependent phosphorylation. LTCC = L-type Ca^{2+}channel, NCX = Na / Ca^{2+} exchanger, β-AR = β-adrenergic receptor, AC = adenylyl cyclase, cAMP = cyclic adenosine monophosphate, Epac = exchange protein directly activated by cAMP, NOS1 = nitric oxide synthase 1, CaMKII = Ca^{2+}/calmodulin-dependent protein kinase II, RyR = ryanodine receptor, SERCA = sarcoplasmic Ca^{2+}-ATPase, PLB = phospholamban.*

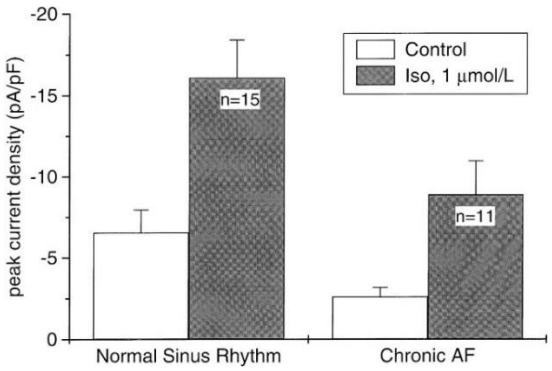

Supplemental figure 2 Responsiveness of AM to β-adrenergic agonist (Isoproterenol; ISO (1 µmol / L)) in chronic AF is not impaired. *Peak current density was measured in AM (n=15) from eight patients in normal sinus rhythm and in AM (n=11) from four chronic AF patients. Data was represented as mean±SEM (Van Wagoner et al. (39)).*

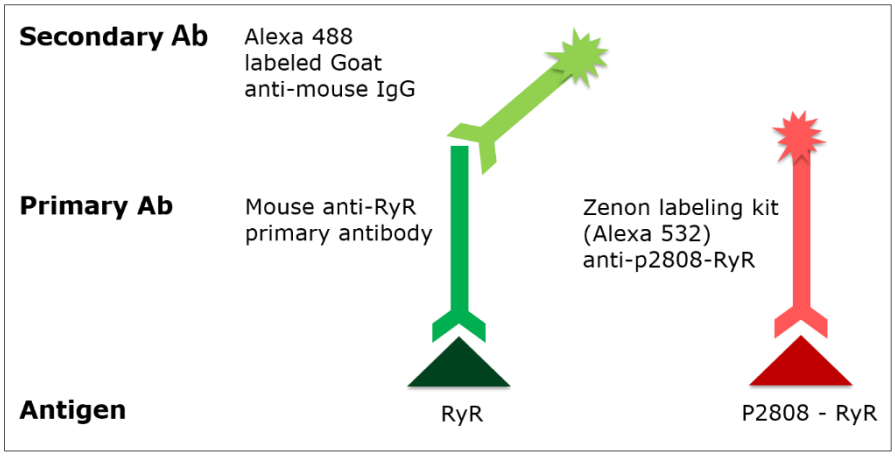

Supplemental figure 3 Scheme of primary and secondary antibody (Ab) use. *Mouse primary Ab was raised in mouse against RyR in rabbits. The primary Ab was recognized by a secondary Alexa 488 labeled goat anti-mouse Ab. In addition, a primary Ab that was already labeled (Alexa 532) was used to target serine 2808 (P2808), the PKA-dependent RyR phosphorylation site.*

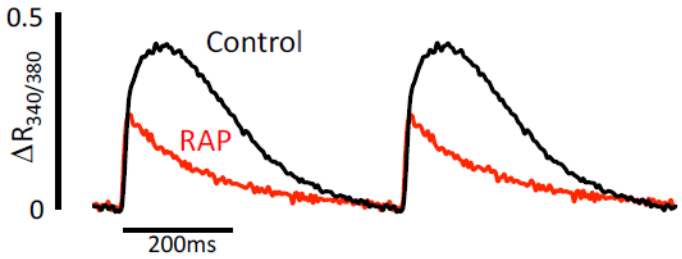

Supplemental figure 4 Reduced baseline Ca^{2+} transient amplitude in a rabbit model of tachy-paced atrial remodeling. *Averaged whole-cell Ca^{2+} transients from control (i.e. SHAM) and RAP cells (n = 10). (Greiser et al. (32)).*

8.2 Supplemental tables

Supplemental table 1 Composition of Solution A (pH = 7.4).

Solution A (2 Liters)	**Concentration [mM]**	**MW**	**g/l**
NaCl	133	58.44	7.7725
KCl	5	74.55	0.372
$MgCl_2 \cdot 6H_2O$	2	203.3	0.4046
KH_2PO_4	1.2	136.09	0.1633
Taurine	6	125.15	0.7509
Creatine	6	131.13	0.7867
Glucose	10	180.16	1.8016
HEPES	10	238.30	2.383

Supplemental table 2 Composition of Solution Enzyme.

Solution Enzyme	**ml or mg**
Solution A	100 mL
$CaCl_2$ (stock solution 100 mM)	0.015 mL
Collegenase P (Roche 11213865)	15 mg
Collegenase B (Roche 11088815)	40 mg
Trypsine inhibitor (Roche 10109878)	7.5 mg
Hyaluronidase (Sigma H-3506)	25 mg

Supplemental table 3 Composition of Solution Storage.

Solution Storage	**ml or mg**
Solution A	100 mL
$CaCl_2$ (stock solution 100 mM)	0.015 mL

Supplemental table 4 Composition of Normal Tyrode solution (pH = 7.4).

Normal Tyrode solution	**Concentration [mM]**	**MW**	**g/l**
NaCl	135	58.44	7.8894
KCl	5	74.55	0.3728
$MgCl_2$	1	95.21	0.0952
$CaCl_2$	1.8	110.98	0.1998
Glucose	10	180.16	1.8016
HEPES	10	238.30	2.383

Supplemental table 5 Composition of Isoproterenol solution (300 nM).

Isoproterenol solution	**ml or mg**
Normal Tyrode solution	50 mL
Isoproterenol (stock solution 10 mM)	0.0015 mL

Auteursrechtelijke overeenkomst

Ik/wij verlenen het wereldwijde auteursrecht voor de ingediende eindverhandeling:
Microdomain-specific beta-adrenergic regulation of calcium signaling in tachycardia-induced atrial fibrillation

Richting: **Master of Biomedical Sciences-Clinical Molecular Sciences**
Jaar: **2018**

in alle mogelijke mediaformaten, - bestaande en in de toekomst te ontwikkelen - , aan de Universiteit Hasselt.

Niet tegenstaand deze toekenning van het auteursrecht aan de Universiteit Hasselt behoud ik als auteur het recht om de eindverhandeling, - in zijn geheel of gedeeltelijk -, vrij te reproduceren, (her)publiceren of distribueren zonder de toelating te moeten verkrijgen van de Universiteit Hasselt.

Ik bevestig dat de eindverhandeling mijn origineel werk is, en dat ik het recht heb om de rechten te verlenen die in deze overeenkomst worden beschreven. Ik verklaar tevens dat de eindverhandeling, naar mijn weten, het auteursrecht van anderen niet overtreedt.

Ik verklaar tevens dat ik voor het materiaal in de eindverhandeling dat beschermd wordt door het auteursrecht, de nodige toelatingen heb verkregen zodat ik deze ook aan de Universiteit Hasselt kan overdragen en dat dit duidelijk in de tekst en inhoud van de eindverhandeling werd genotificeerd.

Universiteit Hasselt zal mij als auteur(s) van de eindverhandeling identificeren en zal geen wijzigingen aanbrengen aan de eindverhandeling, uitgezonderd deze toegelaten door deze overeenkomst.

Voor akkoord,

Cuypers, Anne

Datum: **8/06/2018**